NASA TECHNICAL MEMORANDUM

NASA TM X- 62,320

NASA TM X- 62,320

TAKEOFF AND LANDING PERFORMANCE AND NOISE MEASUREMENTS OF A DEFLECTED SLIPSTREAM STOL AIRPLANE WITH INTERCONNECTED PROPELLERS AND ROTATING CYLINDER FLAPS

James A. Weiberg, Demo Giulianetti,
Bruno Gambucci, and Robert C. Innis

Ames Research Center
Moffett Field, Calif. 94035

December 1973

NOTATION

c	wing chord
C_D	drag coefficient, $\frac{D}{qS}$
C_L	lift coefficient, $\frac{L}{qS}$
C_m	pitching moment coefficient, $\frac{M}{qSc}$
C_Q	torque coefficient, $\frac{Q}{\rho n^2 D^5}$
C_T	thrust coefficient, $\frac{T}{\rho n^2 D^4}$
D	drag and propeller diameter
F	control force
H_p	pressure altitude
HM	control surface hinge moment
J	propeller advance ratio, $\frac{V}{nD}$
L	lift
M	pitching moment
n	propeller rotational velocity
Q	torque
q	free-stream dynamic pressure
R	propeller blade radius
S	area
SHP	shaft horsepower
T	thrust
T_c'	thrust coefficient, $\frac{T}{qS}$
V	airspeed
W	gross weight

α	angle of attack
β	propeller blade angle
γ	flight path angle
δ	movable surface deflection
ρ	mass density of air

Subscripts

A	aft flap
a	aileron
e	elevator
f	main flap
H	horizontal surface
i	indicated
r	rudder
R	right
s	spoiler
ta	aileron spring tab
te	elevator spring tab
tg	geared tab
V	vertical surface
w	wing

TAKEOFF AND LANDING PERFORMANCE AND NOISE MEASUREMENTS OF A DEFLECTED SLIPSTREAM STOL AIRPLANE WITH INTERCONNECTED PROPELLERS AND ROTATING CYLINDER FLAPS

James A. Weiberg, Demo Giulianetti
Bruno Gambucci and Robert C. Innis

Ames Research Center

SUMMARY

A YOV-10A aircraft was modified to incorporate rotating cylinder flaps and interconnected propellers with Lycoming T-53-L11 engines. Flight tests were made to evaluate the low speed handling qualities and performance characteristics. The flight test results indicated that landings could be made with approach speeds of 55 to 65 knots (C_L = 4.5) and descent angles of 6° to 8° for total flap angles of 60° to 75°. At higher flap angles, deterioration of stability and control characteristics precluded attempts at landing. The noise level on the ground under an 8° landing approach path was below 86 PNdB at distances beyond 1 nautical mile from touchdown.

Takeoffs were made with 30° to 45° flaps at lift off speeds of 75 to 80 knots and climb angles of 4° to 8°. Noise levels were below 83 PNdB at 3.5 nautical miles from the start of ground roll.

INTRODUCTION

A YOV-10A aircraft was modified to incorporate an improved propulsion and flap system to provide STOL capability. Flight tests were conducted to evaluate the low speed performance and handling qualities of the modified aircraft. Preliminary results of these tests are presented in reference 1.

Part of the flight evaluation included the effect of flap configuration on landing and takeoff performance and determination of the noise characteristics when operating in the STOL regime. The results of this portion of the investigation are reported herein.

AIRPLANE DESCRIPTION

The research airplane is a twin-engined turbo-propeller North American Rockwell YOV-10A airplane modified to incorporate an improved propulsion system with propeller interconnect and a new flap concept which utilizes a rotating cylinder in the trailing-edge flaps. The airplane is shown in figure 1. The geometry and dimensions are given in figure 2 and table 1. A complete description of the aircraft is given in reference 1.

Rotating Cylinder Flaps

The flaps utilize a rotating cylinder to provide improved turning effectiveness and flap lift. The cylinder forms the leading edge of the flap and is in 4 sections. The axis of the cylinder is fixed relative to the wing and the flap deflects about this axis. The drive system consists of individual direct drive hydraulic motors on each cylinder supplied from cross-shaft driven pumps and with a pilot operated on/off control. Cylinder speed is ground adjustable from 2800 to 7600 rpm for the normal propeller speed of 1250 rpm and was set at 7500 rpm. Wind tunnel tests of the aircraft indicated that this cylinder rpm would provide flow attachment for a 90° flap at speeds up to 70 knots. Total power required to drive the four cylinder segments at this rpm is approximately 30 hp.

The flap is divided into four spanwise segments corresponding to each cylinder segment and includes a slotted aft segment, 13 percent of the wing chord. The relative deflection of these flap segments (both main and aft flap) could be adjusted to provide various combinations of spanwise distribution of flap deflection. In the text and figures, flap angle is the total deflection of the aft flap except in cases where, for clarity, both deflections are given. For example 75° flap is 50° deflection of the main flap and 25° additional deflection of the aft flap or $\delta_f = 50/25$. The geometry and dimensions of the flap are shown in figure 2 and table 1.

Propulsion System

The propulsion system consists of two Lycoming T53-L11 engines driving 9.42 ft. diameter 4-bladed propellers which are interconnected by shafting through the wing leading edge. The engines are coupled to the cross shaft through a gear box and free-wheeling clutch so that either engine can drive both propellers. Each propeller is coupled to the cross shaft through a gear box. Gear ratios are given in table 1. The propellers were built by Curtiss-Wright and used on the Canadair tilt wing CL-84 program and have been modified from 14 ft. to 9.42 ft. by cutting 2.3 ft. off the tips for their use on the YOV-10A airplane. The blades are of foam filled fiberglass construction with steel shanks. The propeller geometry is shown in figure 3(a) and performance in figure 3(b)

Engine exhaust was ducted through the main gear wheel wells in the tail booms. The landing gear was fixed in the down position.

The power management system provides two basic modes of operation; the β (blade angle) mode, and the manual mode. In the β mode, the pilot controls β of both propellers with a single control lever. A throttle servo positions the engine power levers to maintain a preselected propeller rpm. In the manual mode, the throttle servo is turned off and both the β lever and the throttle levers for each engine are manually modulated to obtain the desired power rpm combination.

Flight Controls

The primary flight control systems on the airplane are reversible mechanical controls operating elevator, rudders and ailerons with spoilers and differential propeller pitch.

The pilot's controls are a conventional stick and rudder pedals which operate the controls through a system of bell cranks, push-pull rods, and cables. Nose gear steering is actuated through the rudder pedals.

Longitudinal control is through operation of spring tabs on the elevator which also have geared tabs. Lateral control is through spring tabs on the ailerons and with spoilers and incorporates servo actuated differential propeller pitch $\Delta\beta$ proportional to lateral stick displacement ($\pm$ 4° for maximum displacement). The $\Delta\beta$ system operates only with flaps deflected through a pilot controlled on/off switch. The trim systems incorporate electro-mechanical actuators. Longitudinal and lateral trim are a bungee type; directional trim is with a tab on the left rudder. The geometry of the control systems are given in figure 4 and table 1.

Instrumentation

The flight test data were recorded on an oscillograph and photo recorder in the aircraft. These recorded parameters and the instrumentation displayed on the pilots panel are listed in table II. An FM-FM telemetry system provided ground monitoring of the parameters indicated in table II. For some approaches and landings, either a ground based Bell radar landing approach aid or a pulse coded optical landing aid was used to provide the pilot with flight path indication. The radar system and/or a Fairchild Photographic Flight Analyzer were used to track the aircraft and record flight path data.

The Fairchild Analyzer consisted of a tripod mounted camera which records photographically on a sensitized plate the flight path trajectory of the aircraft. The lens and photographic plate of the camera are fixed relative to the aircraft flight path. Tracking of the moving aircraft manually by the operator moves an optical tracking mechanism with a shutter and aperture which exposes the sensitized plate in a series of pictures abutting each other and providing images of the aircraft spaced along the flight path as shown in figure 5(b).

TEST PROCEDURES AND CONDITIONS

The tests were conducted from either Moffett Field or Crows Landing California. All takeoffs and landings were from a concrete runway at an elevation of approximately 50 ft. (15.24m). The airplane was flown at a takeoff gross weight of 11,582 lb. (5,243 kg) with the c.g. at 22.0 percent chord. Landing gross weight was about 10,860 lb. (4,930 kg).

Noise measurements were made by flying the airplane at constant 70 knots airspeed and 50 foot altitude over an arrangement of microphones set up on the runway. The noise measuring equipment and data reduction and corrections are described in references 2 and 3.

RESULTS AND DISCUSSION

The flight tests included an evaluation of the approaches and landings with various flap deflections. Typical time histories are shown in figure 5(a). The landing approach speeds and descent angles for 60° and 75° flaps are shown in figure 6. Approach speeds of 55 to 65 knots were used with descent angles of 6° and 8°. Generally, without some form of glide slope indication the pilot tended to select the lower values of descent angle (5° to 6°) for approaches. Calculated total landing distance over 50 feet is approximately 1,000 feet. Choice of landing approach speed with high flap deflections was dictated by proximity to stall and a minimum control speed determined by the elevator required to control pitch up. Landings with flap deflections greater than 75° were not attempted because of unstable pitch characteristics, low longitudinal control margins, low directional stability, and lateral instability (ref. 1).

Takeoffs were made with 30° to 45° flaps. Lift off speeds were 75 to 80 knots with climb angles of 4° to 8° depending on power setting. Calculated total takeoff distance over 50 feet is approximately 1200 feet.

Effect of Flap Configuration

To investigate if the longitudinal stability and the trim requirements at low speed could be improved and larger control margins provided while

still maintaining the low speed and descent capability, modifications to the flap configuration were made. The modifications consisted of altering the spanwise distribution of deflection of the 4 span segments for both the main and the aft flap. The flap configurations tested are listed in table III. The results of flight tests to determine the effect of various spanwise distribution of flap deflection on control margin, stability, landing approach speed and descent capability are presented in figures 7 to 15. The best flap configuration, based on longitudinal control margin, approach speed and handling qualities, was with the outboard aft flap fixed at 0° (configuration 4, figure 10). With this configuration, 2 to 3° more down elevator were available for control near the stall and 4 to 6° at approach speeds (figures 13 and 14). The angle of attack and power required for a given airspeed were the same as for the uniform spanwise deflected flap. Stall speeds were 1 to 2 knots higher. Stall approaches for both uniform and modified spanwise flap deflection were characterized by directional wandering and tendency to diverge at low sideslip angles ($\pm$ 5°); 0°sideslip was difficult to hold. Approach to the stall at high flap angles was accompanied by buffett and vibration, pitch up tendency, and reduced pitch control available.

The aircraft with the flap configuration having 20° main flap offset requires, for a given airspeed, 2.5° higher angle of attack or 10° more flap deflection and 5 to 8% more power (figures 9, 11, and 15). This configuration did provide a 2 to 3 knot reduction in speed at which the variation of δ_e with V becomes unstable when compared at flap deflections for the same airspeed/ angle of attack variation (figure 13).

A qualitative evaluation was made of the handling qualities of the aircraft during actual landings for both the symmetrical flap (configuration 1) and with the best modified flap configuration (configuration 4). Touch and go landings were made with these flap configurations for flap deflections of 60° and 75°. The approaches were made tracking an 8° glide slope. Typical radar traces and Fairchild camera records of the aircraft flight path are shown in figure 5. Average landing approach speeds varied from 55 knots for the 75° symmetrical flap to 60 knots for the modified flap. A summary of the pilots qualitative analysis and comments on these landings is given in the following section.

Pilot's Comments on Landing Handling Qualities

The following comments are primarily directed at the landings made with the modified flap. However, the comments also apply to flights with the symmetrical flap particularly with regard to ability to track glide slope and arrest sink rate. Approaches for these flights were made on an 8° glide slope provided by either an ILS or a pulse coded optical landing aid. Winds were light (3 - 5 knots) and turbulence was light to moderate.

The pilot commented that glide slope tracking was not too bad but it seemed more difficult to correct from a low approach than from a high. The aircraft response to β lever steps seemed very slow probably because of the large prop rpm excursions that occurred (figure 16). Minimum approach speed was dictated by the desire not to exceed 15° indicated angle of attack. In smooth air the pilot was willing to approach at 15° but in turbulence would back off to minimise excursions above 15°. Glide slope tracking

seemed to deteriorate somewhat at the minimum approach speed. Other than slightly different thrust required and different approach speeds, no appreciable difference was noted between 60° and 75° flap. Low static longitudinal stability did not seem to present a big problem. The biggest contribution to pilot workload was probably the lateral axis. The aircraft is easily disturbed in turbulence (low stability, high dihedral effect) and although sideslip excursions didn't seem very large, the roll motion was objectionable. Rather large and frequent lateral stick motion was required to correct the disturbance (figure 5(a)). Roll control sensitivity is too low. (Differential β was engaged for all approaches). If the sink rate appeared too high before initiating the flare, as might occur when correcting for a late high on glide slope, an open loop β lever step was made to reduce it. Rotation angles to flare were quite large and the results were inconsistant. Sometimes most of the sink rate was arrested and sometimes little or none of it was. There never was any tendency to float. The pilot had the impression that flare capability might be quite sensitive to airspeed (C_L) at flare initiation. None of the landings were uncomfortable.

Effect of Flight Path on Noise Signature

Measurements were made of the noise generated by the aircraft while flying at an airspeed of 70 knots over the runway at an altitude of 50 feet. The instrumentation and methods used to measure, reduce and correct this data are described in references 2 and 3. Typical sound pressure level frequency spectrums from these noise measurements are presented in figure 17.

These data were then used to compute the noise signatures on the ground in the form of lines of constant noise level as generated by the aircraft during takeoff and landing approach. Noise signatures were computed for a takeoff with 30° flaps and a landing with 75° flaps on an 8° flight path. Time histories are shown in figure 18.

The computer program used to compute the ground noise signatures essentially "flies" the aircraft along the specified flight profile and extrapolates the peak noise produced by the aircraft to a point on the ground. The extrapolation from the flight measured noise data was by applying spherical divergence and atmospheric attenuation over the computed noise propagation distance from the aircraft flight path to the ground.

Typical resulting noise foot prints are presented in figure 19 showing lines of constant noise level located relative to the runway centerline and the end of the runway. For an 8° glide slope, the level of noise heard by an observer on the ground underneath the approach flight path is below 86 PNdB at distances beyond 1 nautical mile from touchdown. Noise level on takeoff with an 8° climb angle was below 83 PNdB at 3.5 nautical miles from the start of ground roll.

CONCLUDING REMARKS

These studies have shown that the rotating cylinder flap concept can be an effective high lift device to provide the low speeds and steep descent angles required for STOL performance. The deterioration of aircraft stability, control, and handling qualities as approach speeds are reduced results from the attempt to operate at the low speeds and high lift coefficients rather than being inherent in the rotating cylinder flap design.

This flap has provided the capability for these problems to be investigated on a small propulsive lift aircraft. The flap is relatively mechanically simple and quiet and provided trouble free operation for over 80 hours of wind tunnel and flight tests.

REFERENCES

1. Cichy, D. R.; Harris, J. W.; MacKay, J. K.L.;Flight Test of a Rotating Cylinder Flap on a North American Rockwell YOV-10 Aircraft. NASA CR 2135, November 1972.

2. Atencio, A.; and Soderman, P.: Comparison of Wind Tunnel and Flyover Noise Measurements of the YOV-10A STOL Aircraft. NASA TM X-62,166 June 1972.

3. Anon.: In-Flight Sound Measurements on the XV-5B and OV-10 Aircraft. Prepared for NASA under Contract NAS2-5462 by General Electric Co., April 1972.

TABLE I - GEOMETRIC DIMENSIONS OF THE AIRPLANE

Wing	
Area, sq. ft. (sq m)	244 (22.67)
Span, ft. (m)	34 (10.36)
Chord, ft. (m)	7.27 (2.21)
Aspect ratio	4.74
Section	64_2A-315 (mod.)
Incidence, deg.	3.0
Horizontal tail	
Area, sq. ft. (sq m)	70 (6.50)
Span, ft. (m)	13.58 (4.14)
Chord, ft. (m)	5.18 (1.58)
Aspect ratio	2.62
Section	Inverted 64_1A412 (mod.)
Tail length, ft. (m)	19.83 (6.04)
Incidence, deg.	4.0
Vertical tail	
Area, sq. ft. (sq m) (each)	35.69 (3.31)
Span, ft. (m)	7.34 (2.24)
Chord, ft. (m)	4.87 (1.48)
Aspect ratio	1.51
Section	64_1A012
Elevator	
Span, ft. (m)	12.97 (3.95)
Maximum deflection, deg.	35 up 20 down
Chord aft of hinge line (c_e/c_H)	.28
forward of hinge line (c_{eb}/c_H)	.043
Tabs (4) (chord/span, ft. (m)(each)	.33/3.24 (.10/.99)
geared tab ratio (S_{t_g}/S_e)	-.80

Aileron (data for one aileron)

Span, ft. (m)	4.02 (1.22)
Maximum deflection, deg.	±25
Chord, aft of hinge line (c_a/c_w)	.20
forward of hinge line (c_{a_b}/c_w)	.06
Tabs (chord/span, ft. (m))	.33/2.84 (.10/.86)
Differential propeller pitch for maximum control, deg.	± 4

Spoilers (Four disk plate type, data for one side)

Span, ft. (m)	3.82 (1.16)
Location % wing chord	59.56
span sta. in. (m)	97.0-143.3 (2.46-3.64)
Projection % wind chord	8.7
area, sq. ft. (sq m)	14.8 (1.37)

Rudder (data for one rudder)

Span, ft. (m)	6.01 (1.83)
Maximum deflection, deg.	± 25
Chord, aft of hinge line (c_r/c_v)	.30
forward of hinge line ($c_{r_b} c_v$)	.10

Engine

Make	Lycoming T53 L 1
Power ratings (hp)	
Takeoff (5 min. limit)	1100
Military (30 min. limit)	1000
Normal (continuous)	900
Gear ratios	
Power turbine to output shaft	3.21:1
Cross shaft gear box input to prop shaft	5:1

Propellers

Make	Curtiss Wright 1490A2P3/4-55
Diameter, ft. (m)	9.42 (2.87)
Number of blades	4
Activity factor/blade	149.9
Disk area, each propeller, sq. ft. (sq m)	69.69 (6.47)
Solidity	.222

Moments of Inertia

Gross weight, lb. (kg)	11,582 (5,253)
Ixx, slug ft^2 (kg m^2) (roll)	12,440 (16,866)
Iyy, slug ft^2 (kg m^2) (pitch)	13,740 (18,629)
Izz, slug ft^2 (kg m^2) (yaw)	24,240 (32,865)
Ixz, slug ft^2 (kg m^2)	2,060 (2,793)

TABLE II - INSTRUMENTATION

Oscillograph

1. L/H prop blade angle
2. R/H prop blade angle
3. L/H throttle position
4. R/H throttle position
5. L/H eng. oil press.
6. R/H eng. oil press.
7. L/H eng. torque
8. R/H eng. torque
9. R/H flap position
10. L/H flap support acc.
11. R/H flap support acc.
12. Normal acc. at cg (z)
13. Long. acc. at cg (X)
14. Lat. acc. at cg (y)
15. Pitch angle
16. Bank angle
17. Angle of attack
18. Angle of sideslip
19. Pitch rate
20. Roll rate
21. Yaw rate
22. Long. stick position
23. Lat. stick position
24. L/H Elevator position
25. L/H Aileron position
26. L/H spoiler position
27. L/H rudder
28. Long. trim position
29. Lat. trim position
30. Dir. trim position
31. L/H EGT
32. R/H EGT
33. Airspeed
34. OAT
35. Tail dynamic pressure
36. Tail downwash

Photo panel

1. Altitude
2. Airspeed
3. L/H prop rpm
4. L/H eng. rpm
5. R/H eng. rpm

Telemetry

1. Airspeed
2. Altitude
3. Angle of attack
4. Pitch angle
5. Bank angle
6. Elevator position
7. Aileron position
8. L/H eng. torque
9. R/H eng. torque
10. Flap support acc.
11. Cylinder brg. temp.

Pilots panel

1. L/H Engine rpm N1
2. R/H Engine rpm N1
3. Prop rpm
4. L/H Engine EGT
5. R/H Engine EGT
6. L/H Engine torque
7. R/H Engine torque
8. Cylinder rpm, 1 and 2
9. Cylinder rpm, 3 and 4
10. Angle of attack
11. Angle of sideslip
12. Airspeed
13. Pressure altitude
14. L/H Engine output turbine rpm N2
15. R/H Engine output turbine rpm N2

TABLE III - FLIGHT DESCRIPTION

Flight	Configuration	Flap Deflection		Gross Weight		c.g	
		Inboard	Outboard	Takeoff	Land	Takeoff	Land
43	2	30/0 40/0 50/0 60/0	30/15 40/20 50/25 60/30	11,582	10,790	22.0	20.8
44	3	40/20 50/25 60/30	20/10 30/15 40/20	11,582	10,736	22.0	20.7
45	4	30/15 40/20 50/25 60/30	30/0 40/0 50/0 60/0	11,582	10,682	22.0	20.6
46	5	40/20 50/25 60/30	20/0 30/0 40/0	11,582	10,790	22.0	20.8
47	6	30/0 40/0 50/0 60/0	30/0 40/0 50/0 60/0	11,582	10,826	22.0	20.9
48	1	30/15 40/20 50/25 60/30	30/15 40/20 50/25 60/30	11,582	10,808	22.0	20.8
50	4	40/20 50/25 50/25	40/0 50/0 50/0	11,132 10,646 11,582	10,646 10,466 11,312	21.3 20.6 22.0	20.6 20.3 21.6

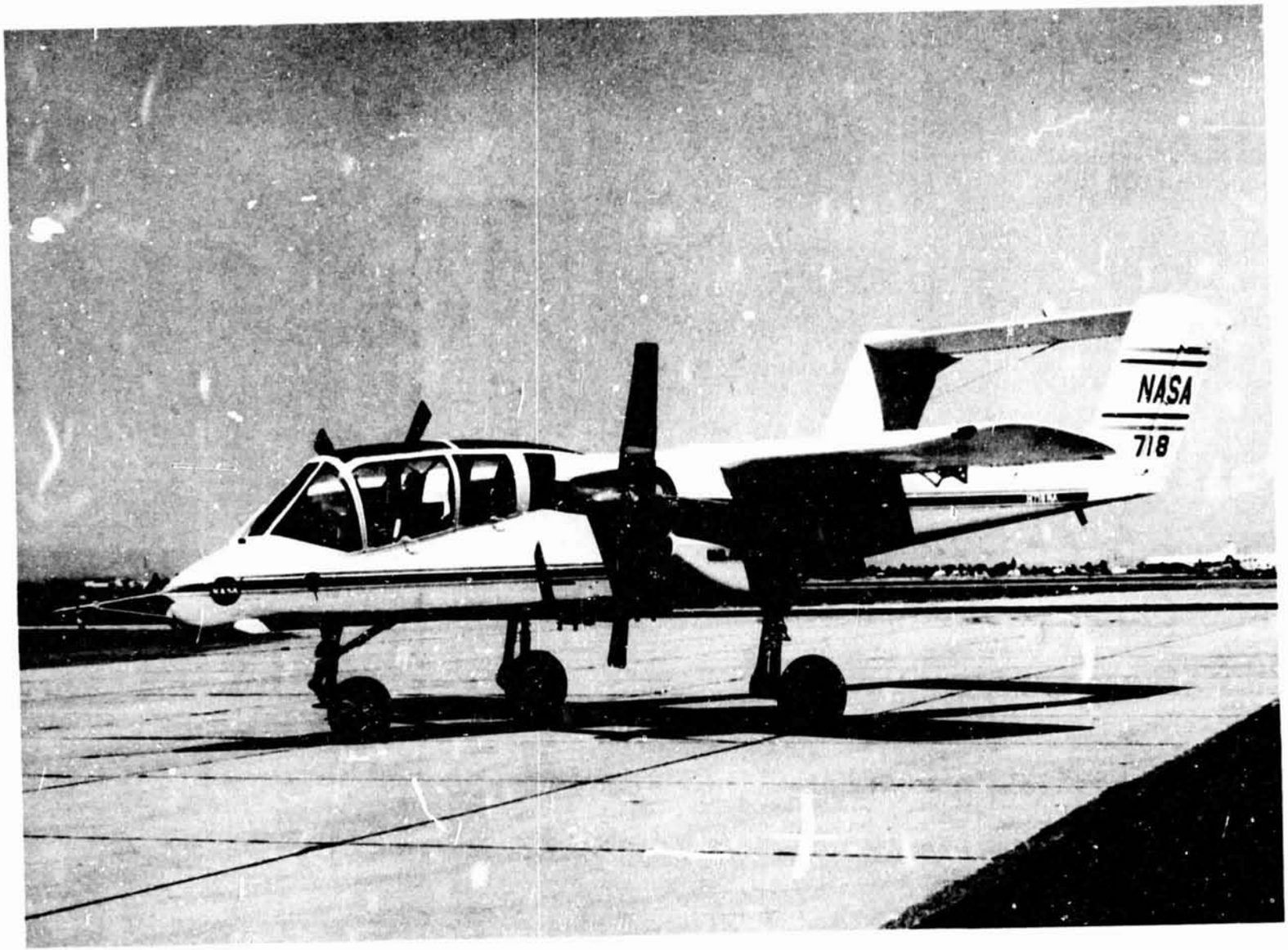

(a) 3/4 front view, flaps up.

Figure 1.-The Airplane.

National Aeronautics and Space Administration
Ames Research Center
Moffett Field, Calif

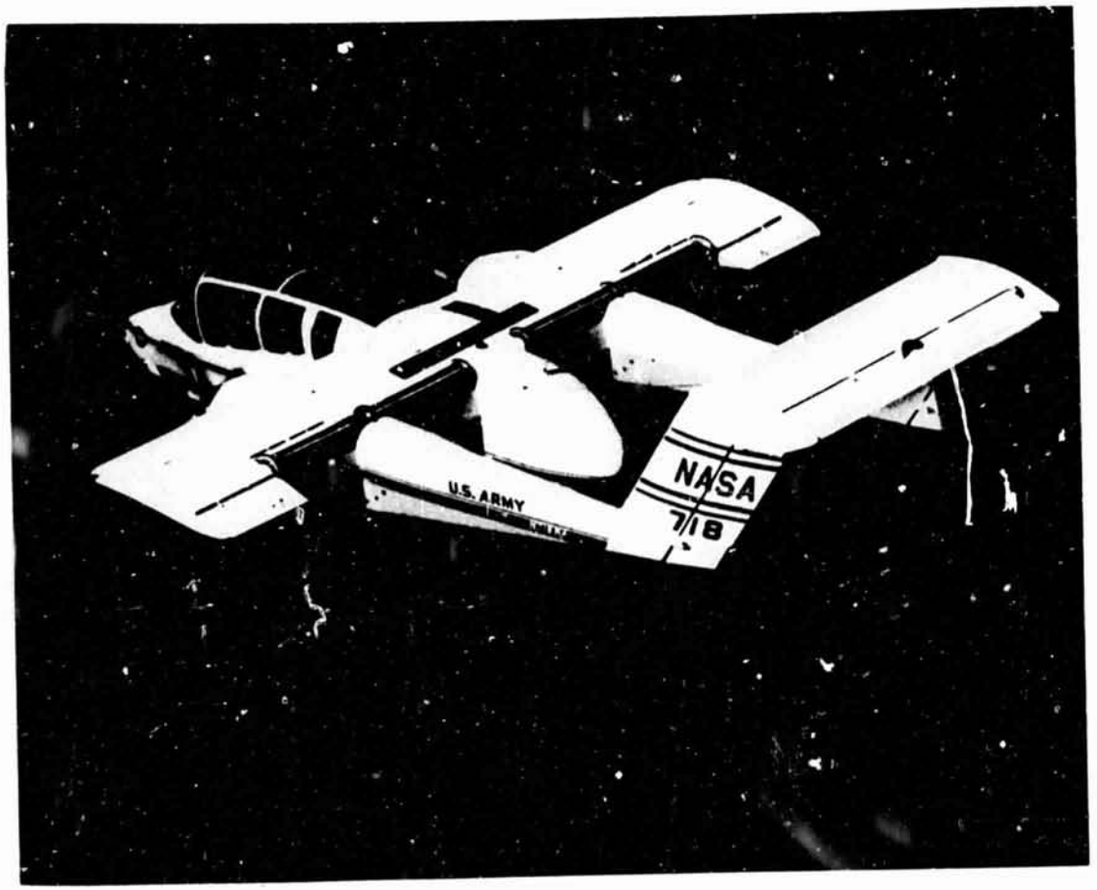

(b) 3/4 rear view flaps down.

Figure 1.-Concluded.

National Aeronautics and Space Administration
Ames Research Center
Moffett Field, Calif

WING

SPAN	34 FT (10.56 m)
AREA	244 SQ FT (22.67 sq m)
CHORD	7.27 FT (2.21 m)
ASPECT RATIO	4.74
SECTION	64_2A-315 (MOD.)
PROPELLER DIA.	9.42 FT (2.87 m)
ENGINES	LYCOMING T53-L11

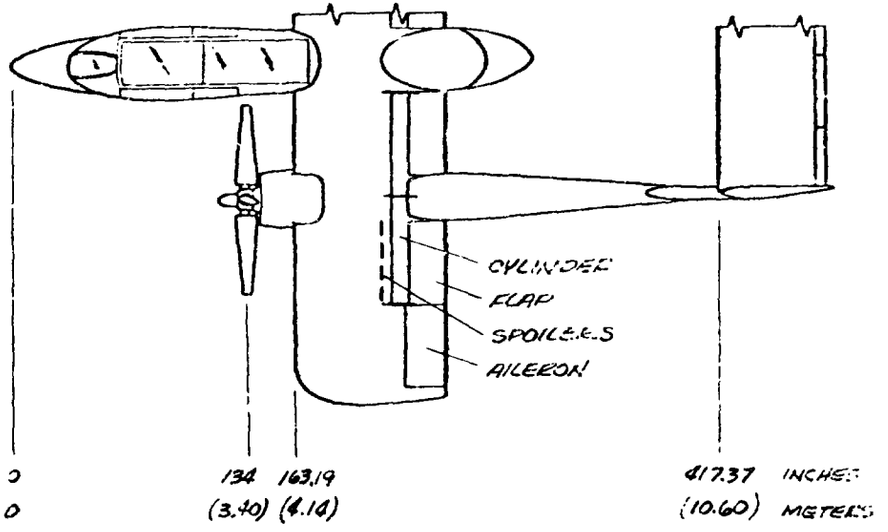

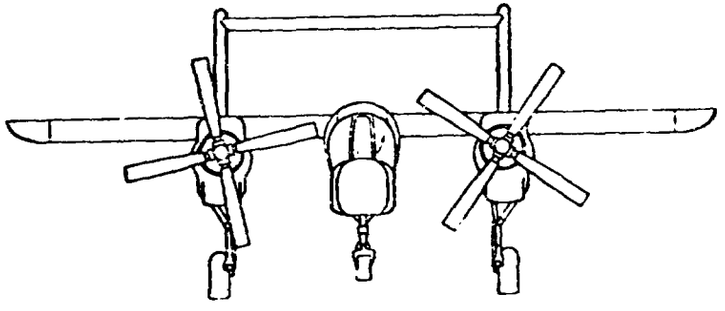

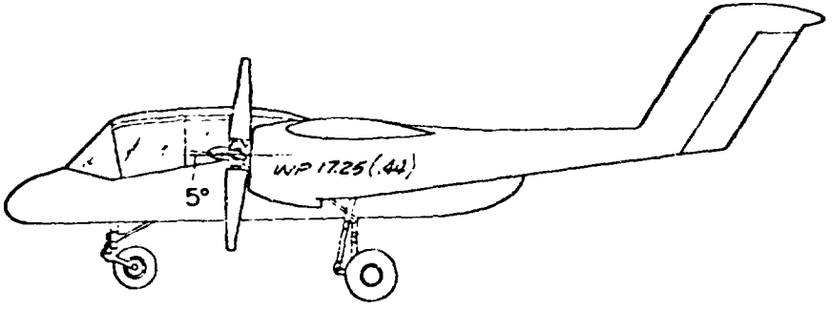

(a) 3 VIEW

FIGURE 2.- GEOMETRY OF THE AIRPLANE.

National Aeronautics and Space Administration
Ames Research Center
Moffett Field, Calif

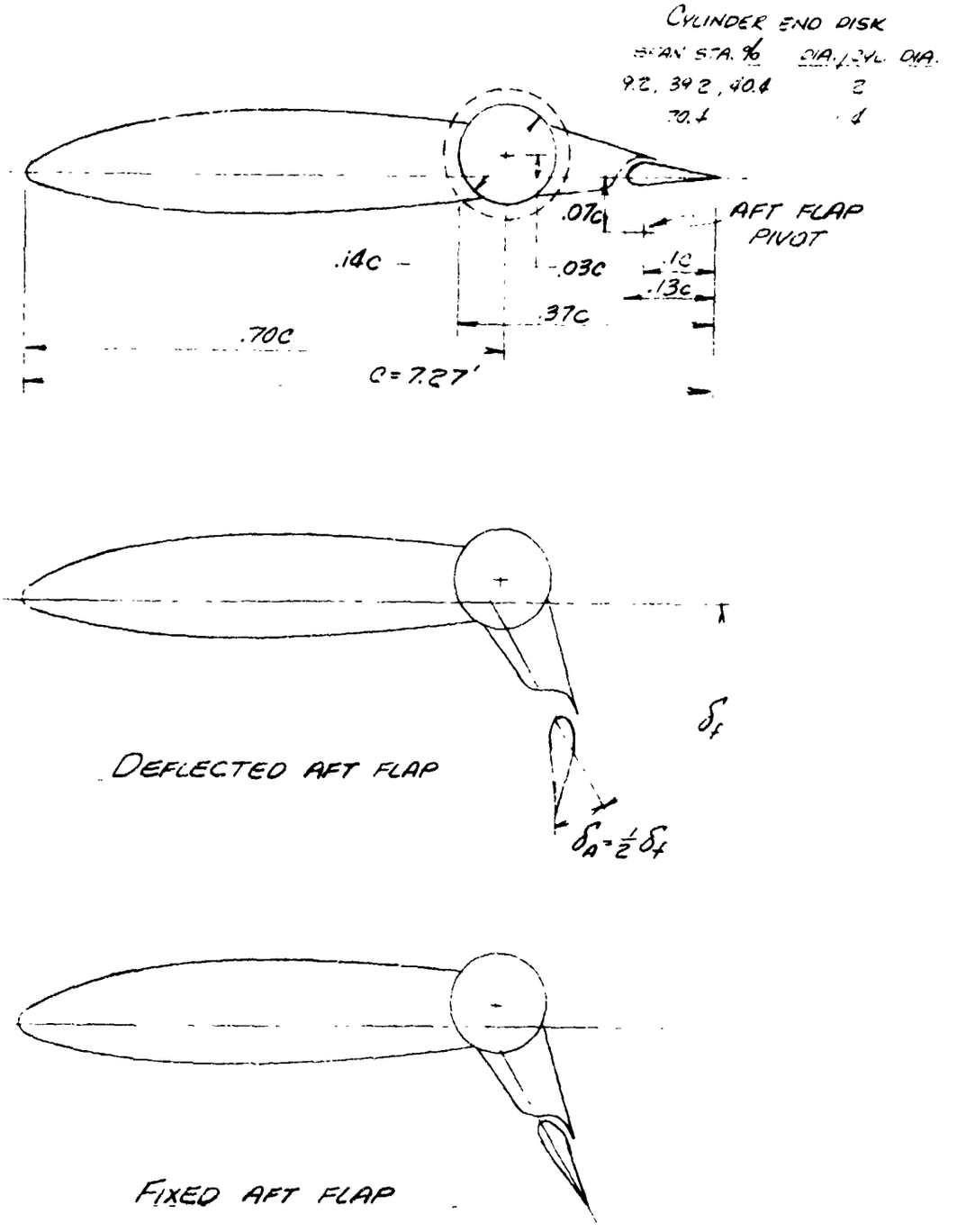

(b) FLAP GEOMETRY

FIGURE 2.- CONCLUDED.

National Aeronautics and Space Administration
Ames Research Center
Moffett Field, Calif

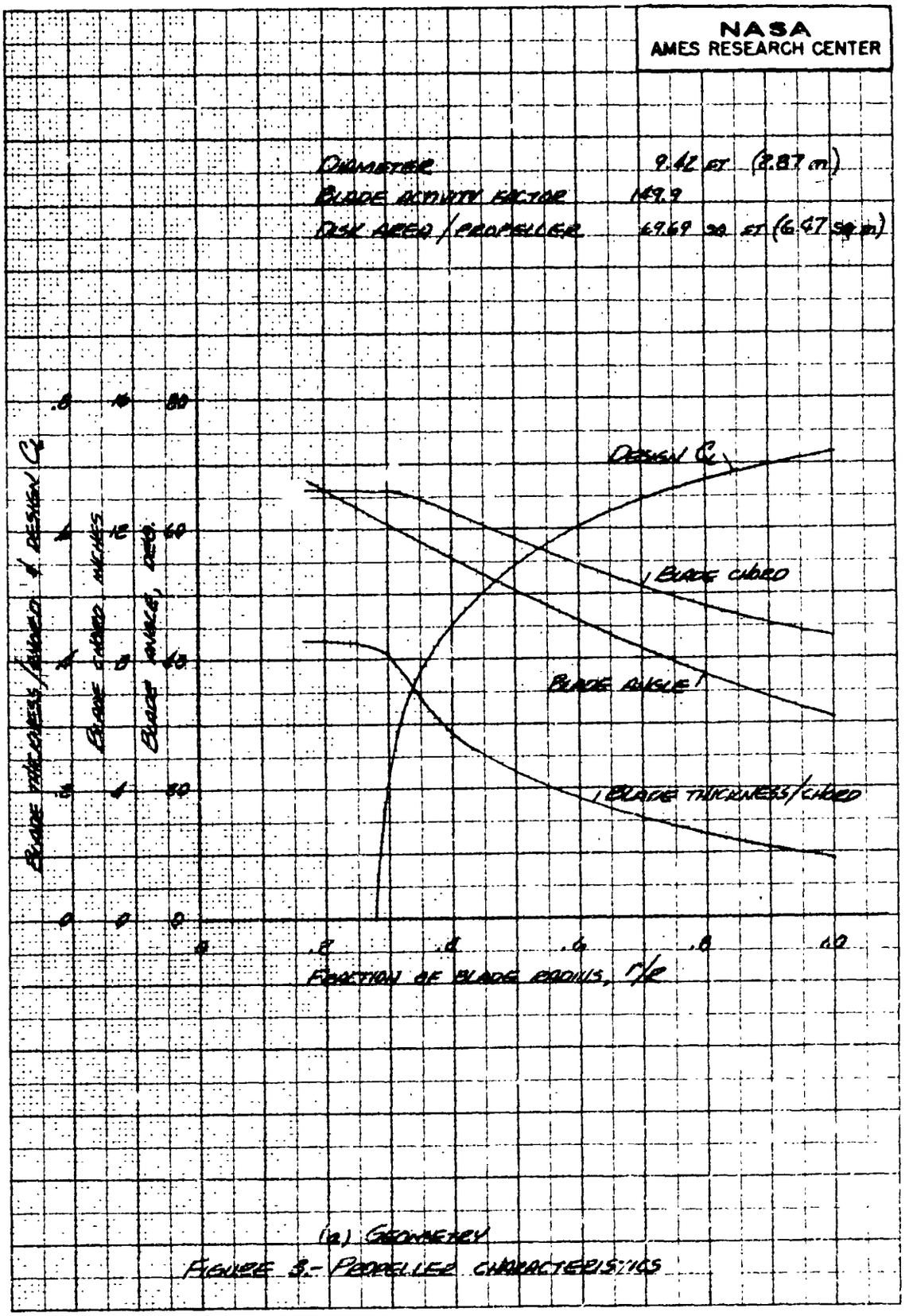

(a) GEOMETRY

FIGURE 3.- PROPELLER CHARACTERISTICS

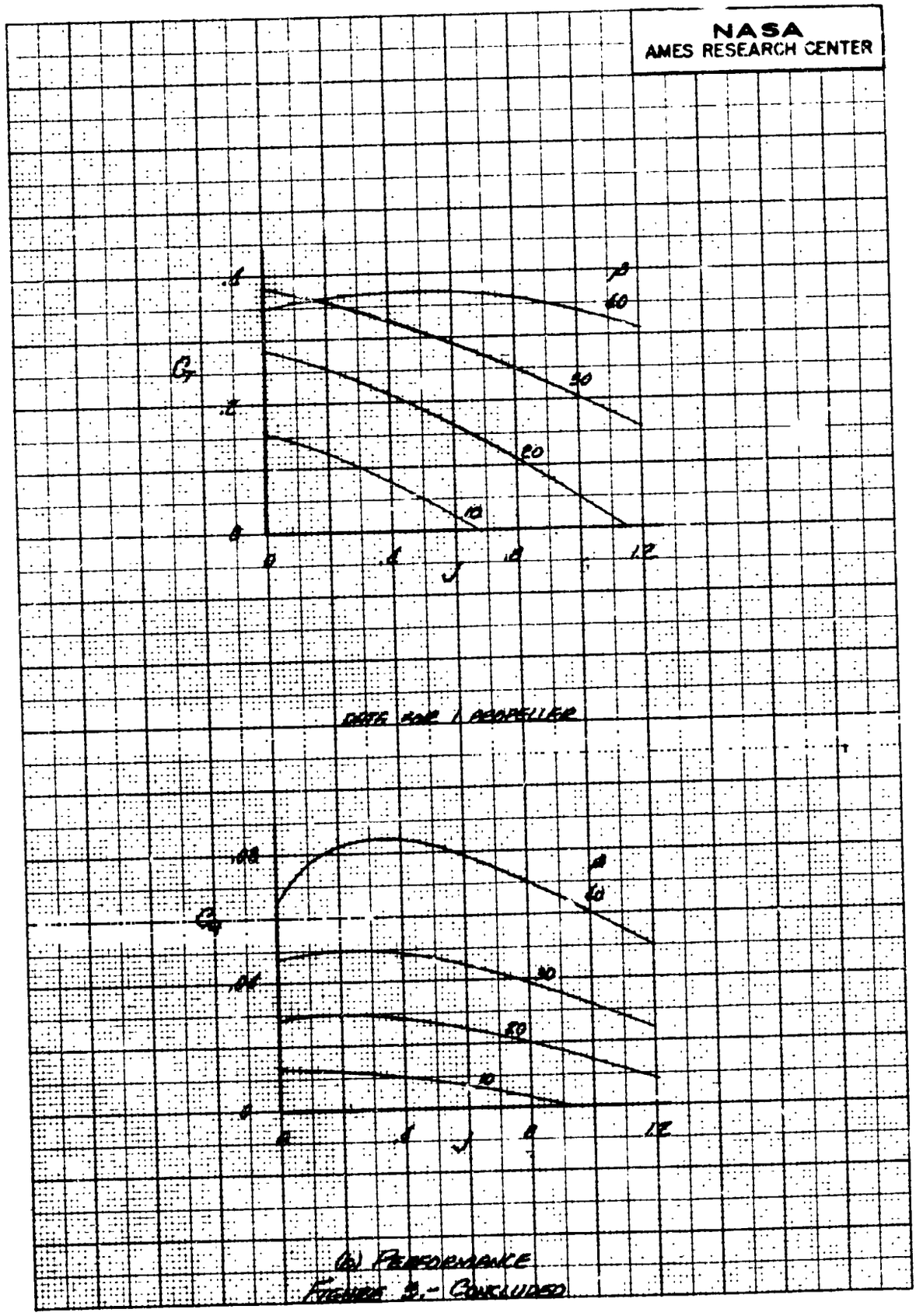

(b) PERFORMANCE

FIGURE 3.- CONCLUDED

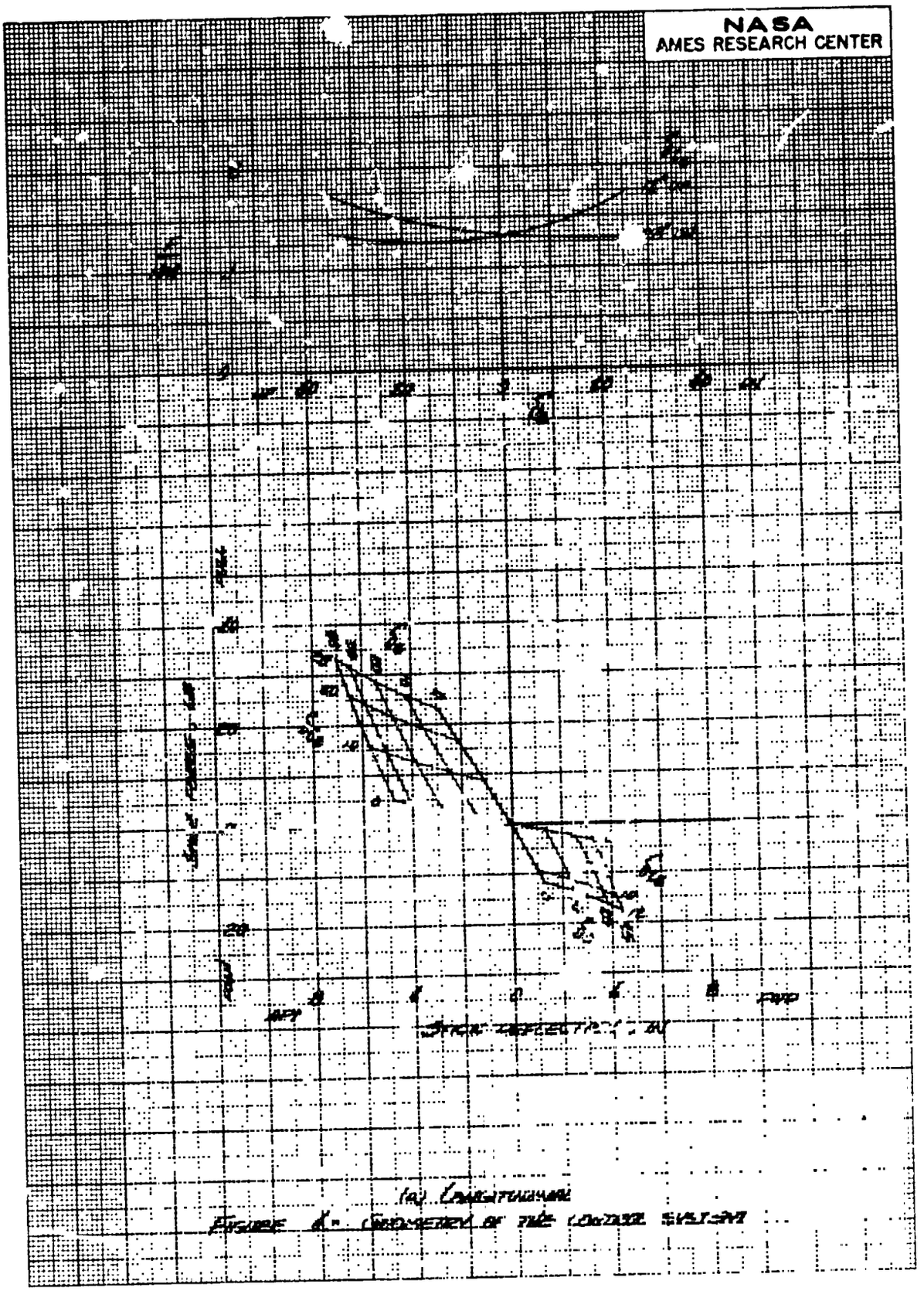

(a) Longitudinal

FIGURE 4.- CONCLUDED

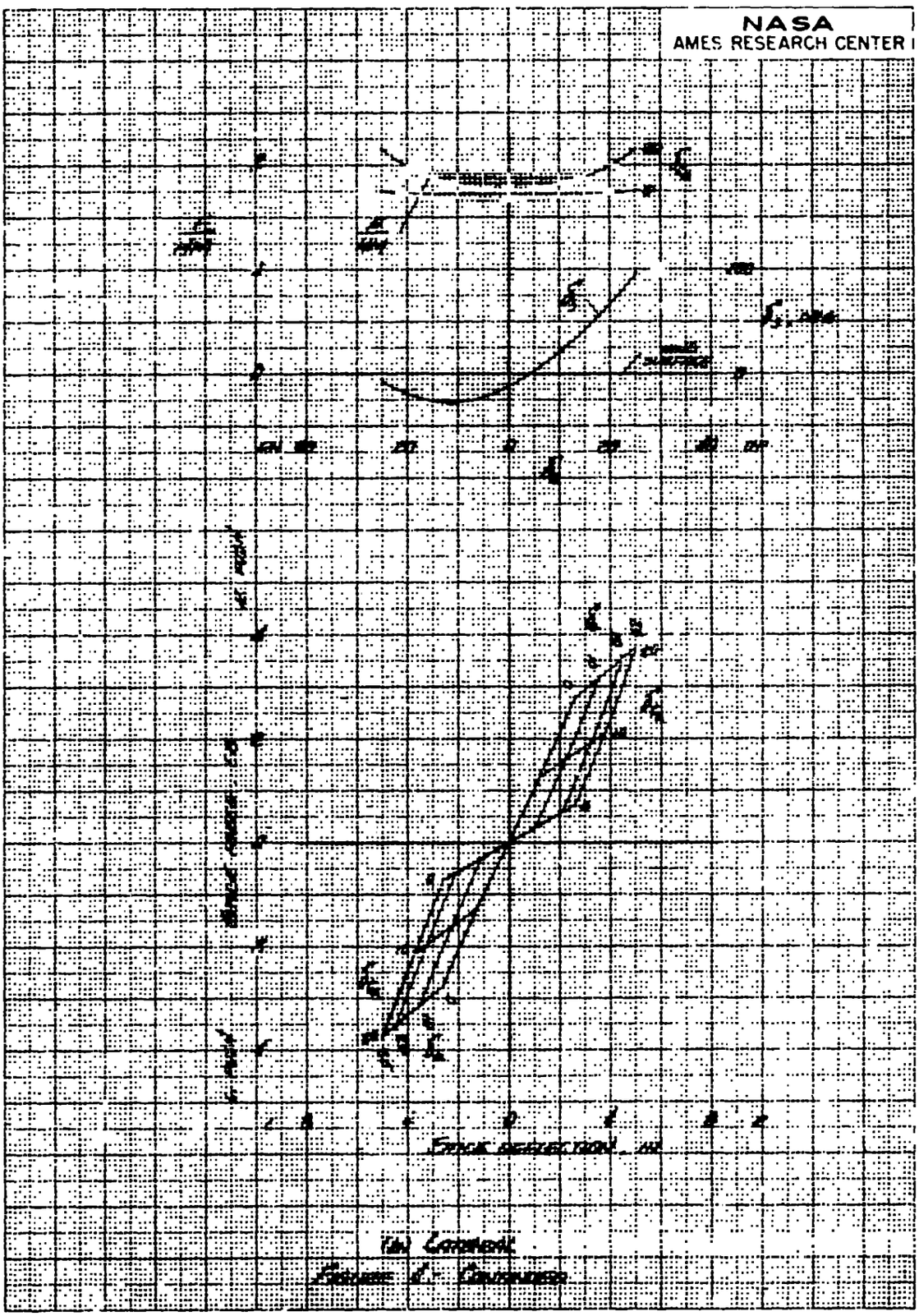
NASA
AMES RESEARCH CENTER

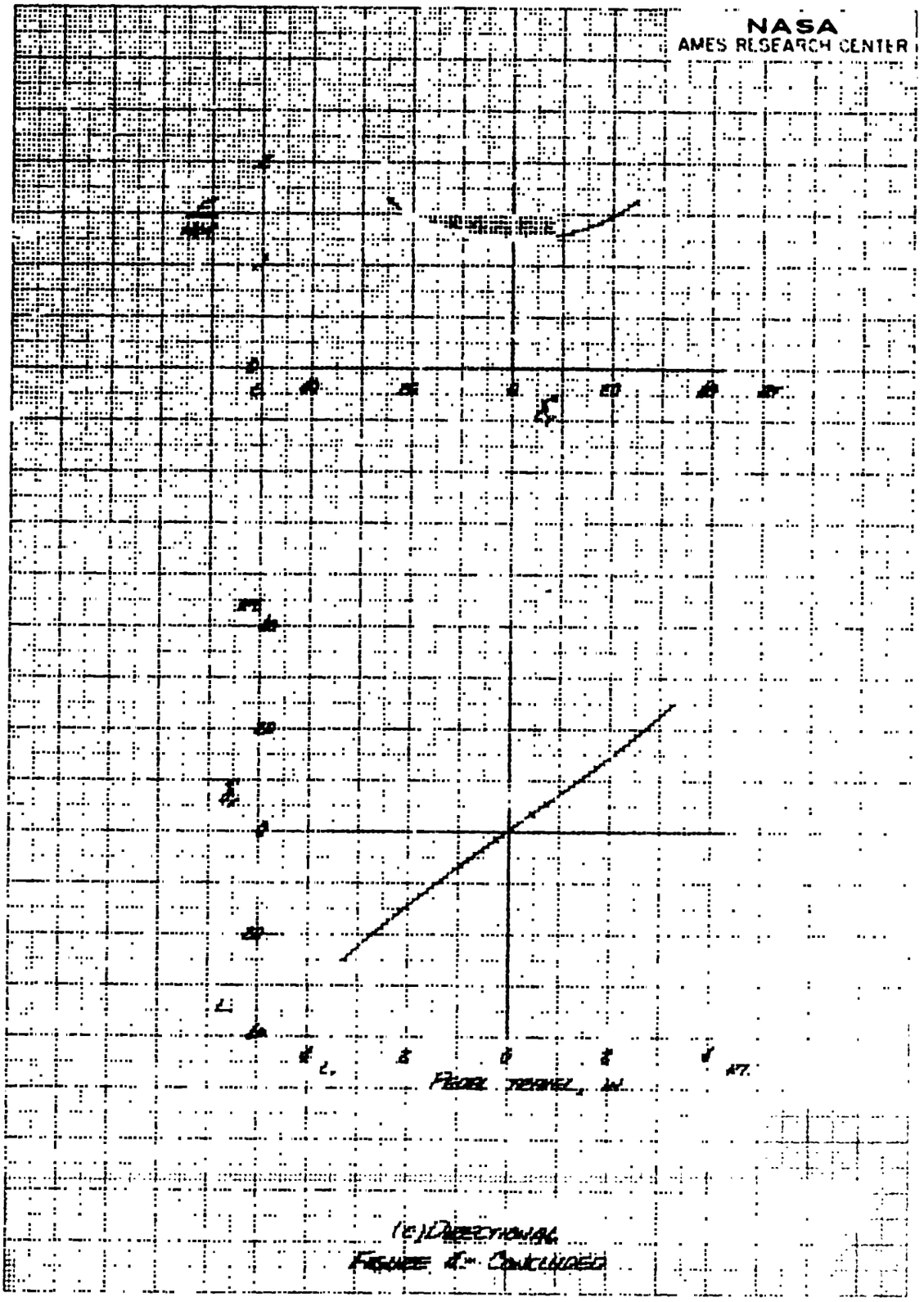
NASA
AMES RESEARCH CENTER

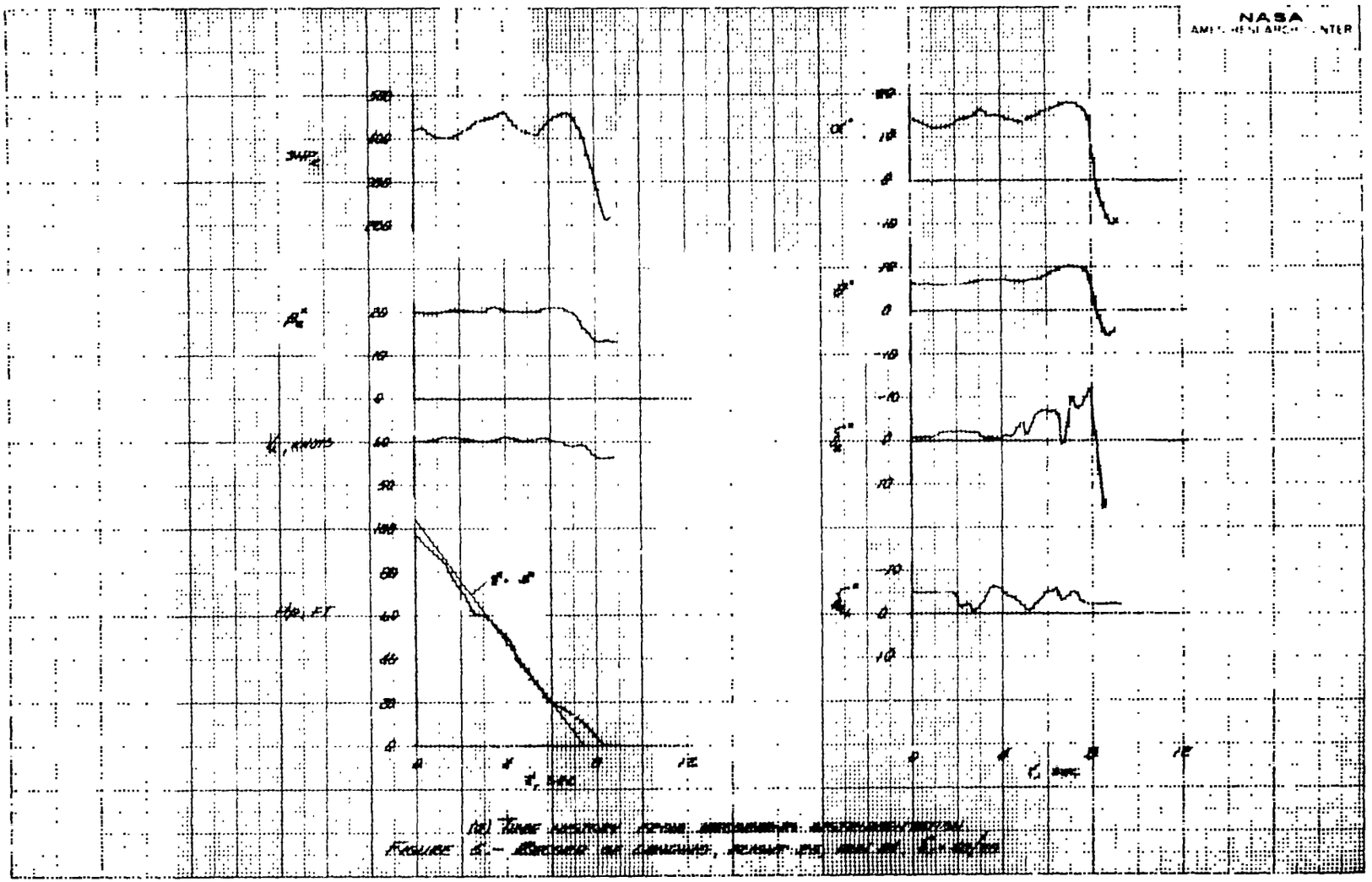
NASA

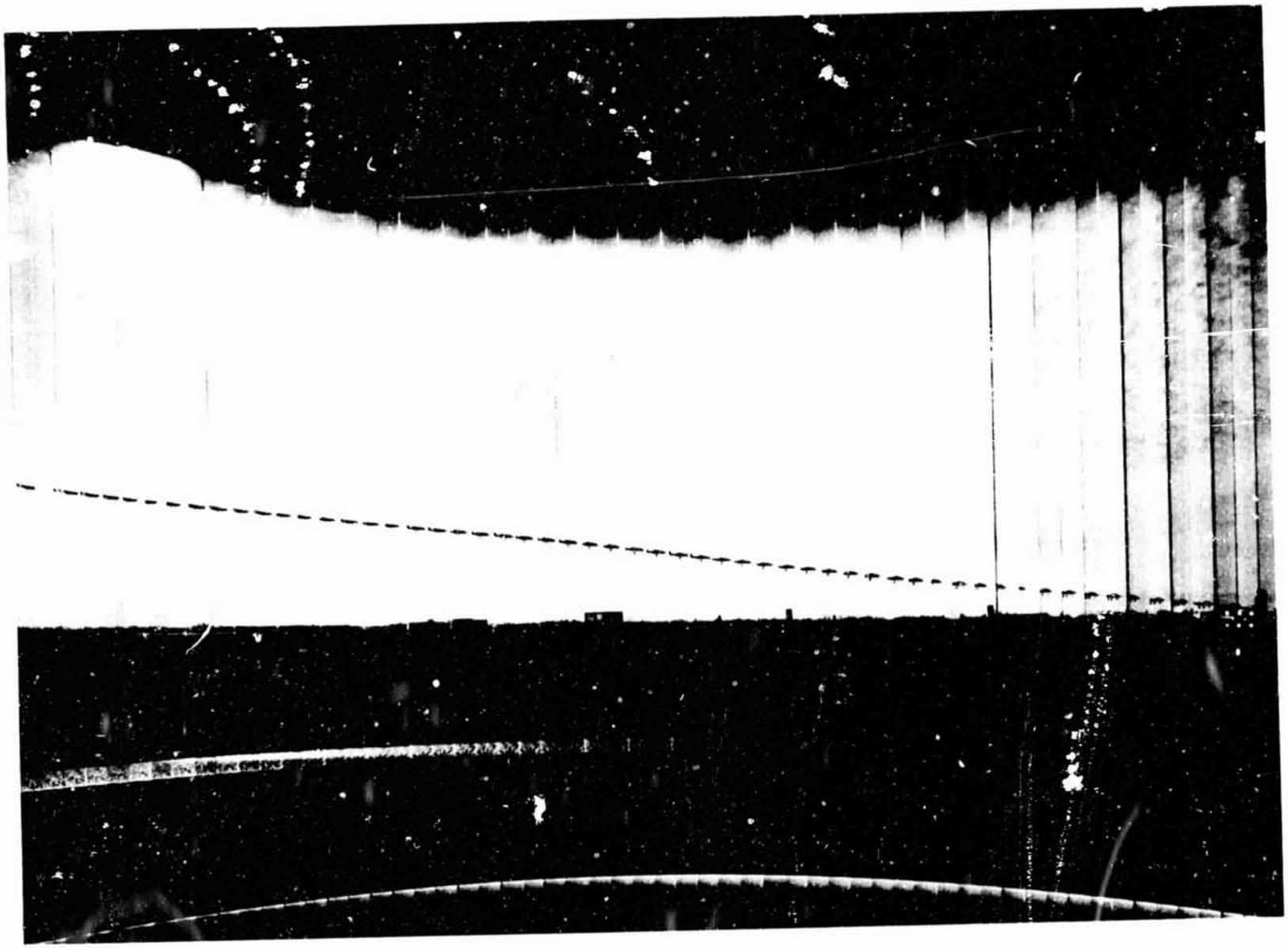

(b) Landing path from Fairchild camera.

Figure 5.-Continued.

National Aeronautics and Space Administration
Ames Research Center
Moffett Field, Calif

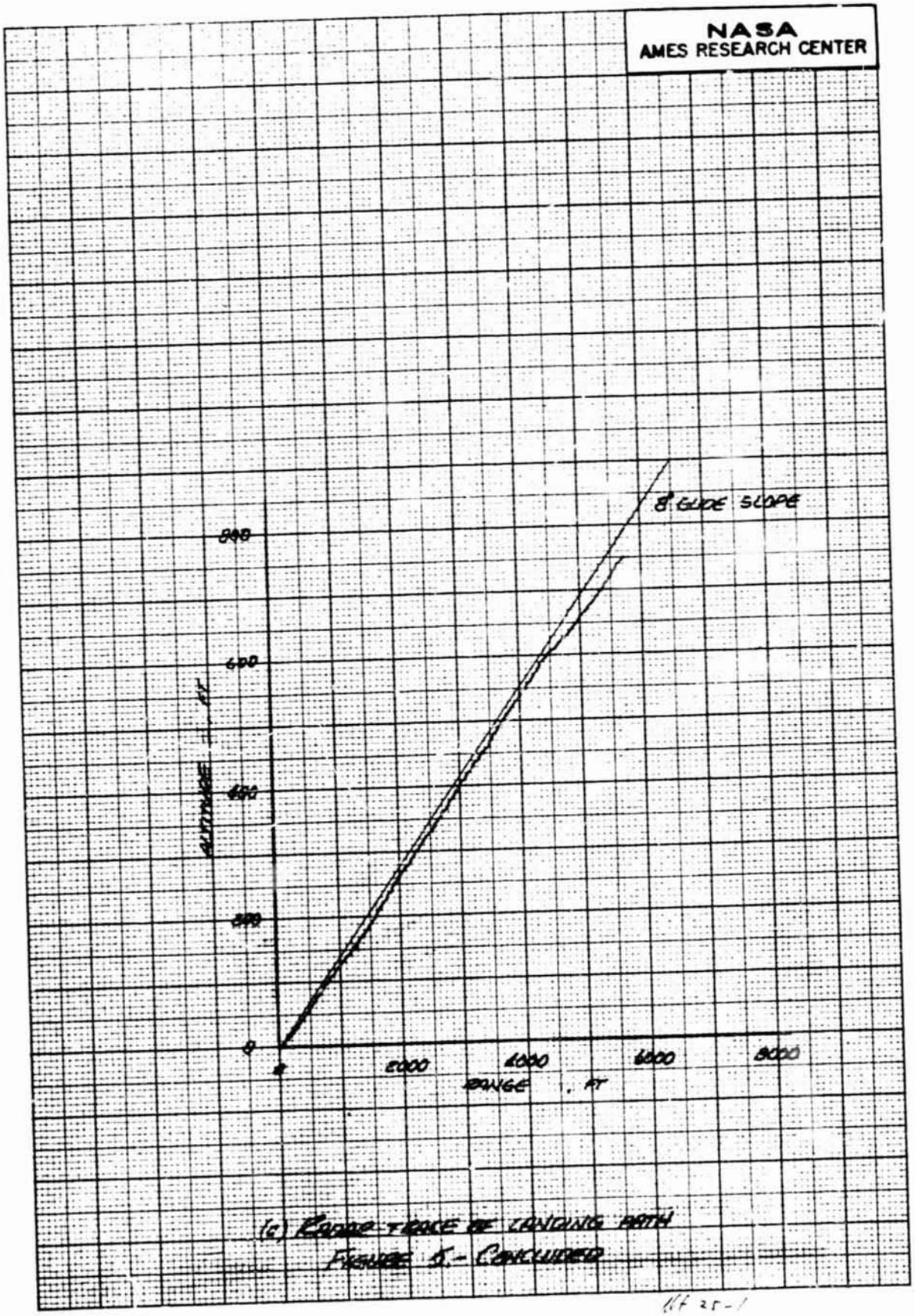

(c) RANGE-HEIGHT OF LANDING PATH

FIGURE 5.- CONCLUDED

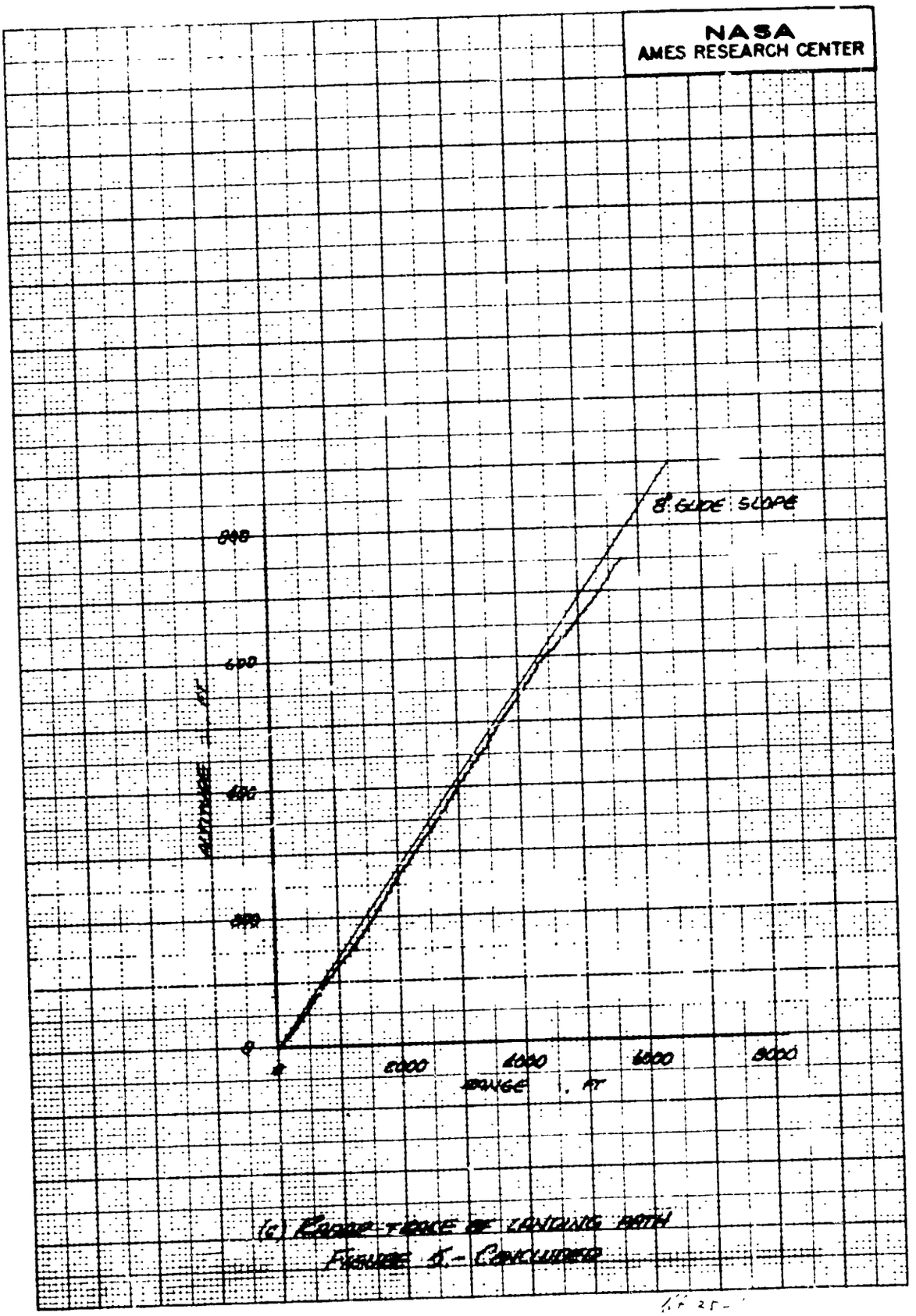

(c) RADAR TRACE OF LANDING WITH FIGURE 5. - CONCLUDED

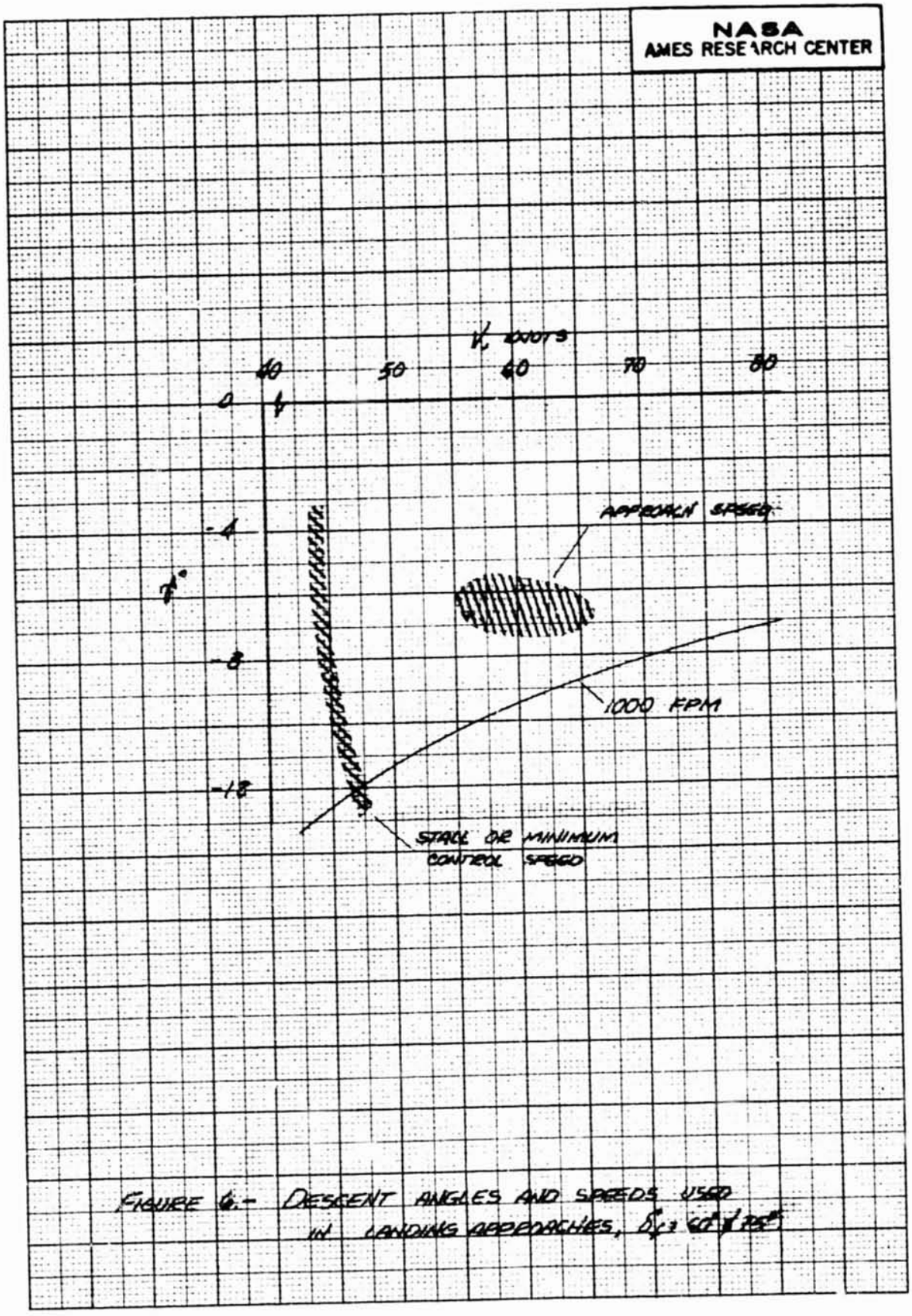

FIGURE 6.- DESCENT ANGLES AND SPEEDS USED IN LANDING APPROACHES, $\delta_f = 60°$ AND $75°$

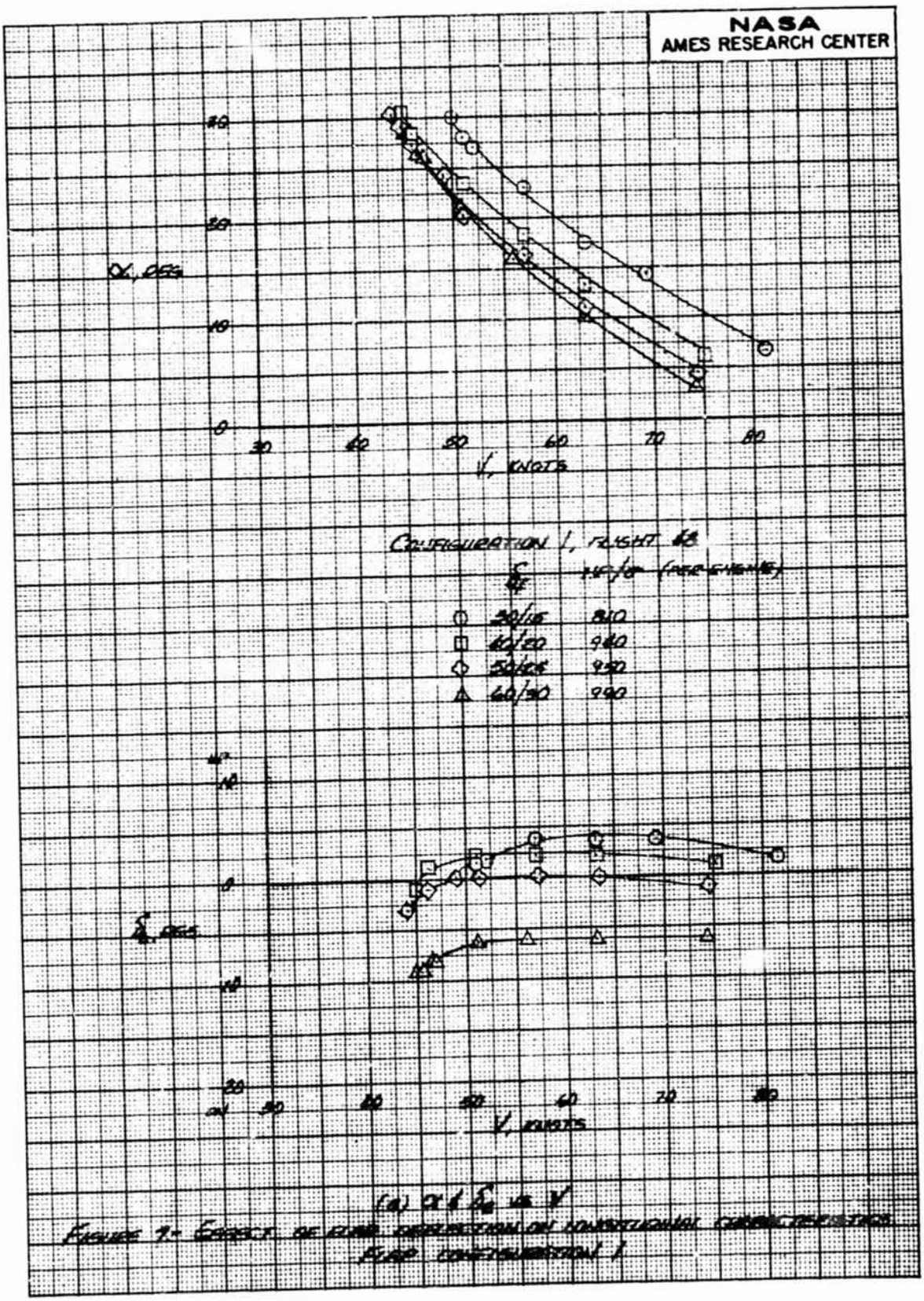

(a) α & δ_e vs V

FIGURE 7.- EFFECT OF FLAP DEFLECTION ON LONGITUDINAL CHARACTERISTICS. FLAP CONFIGURATION 1

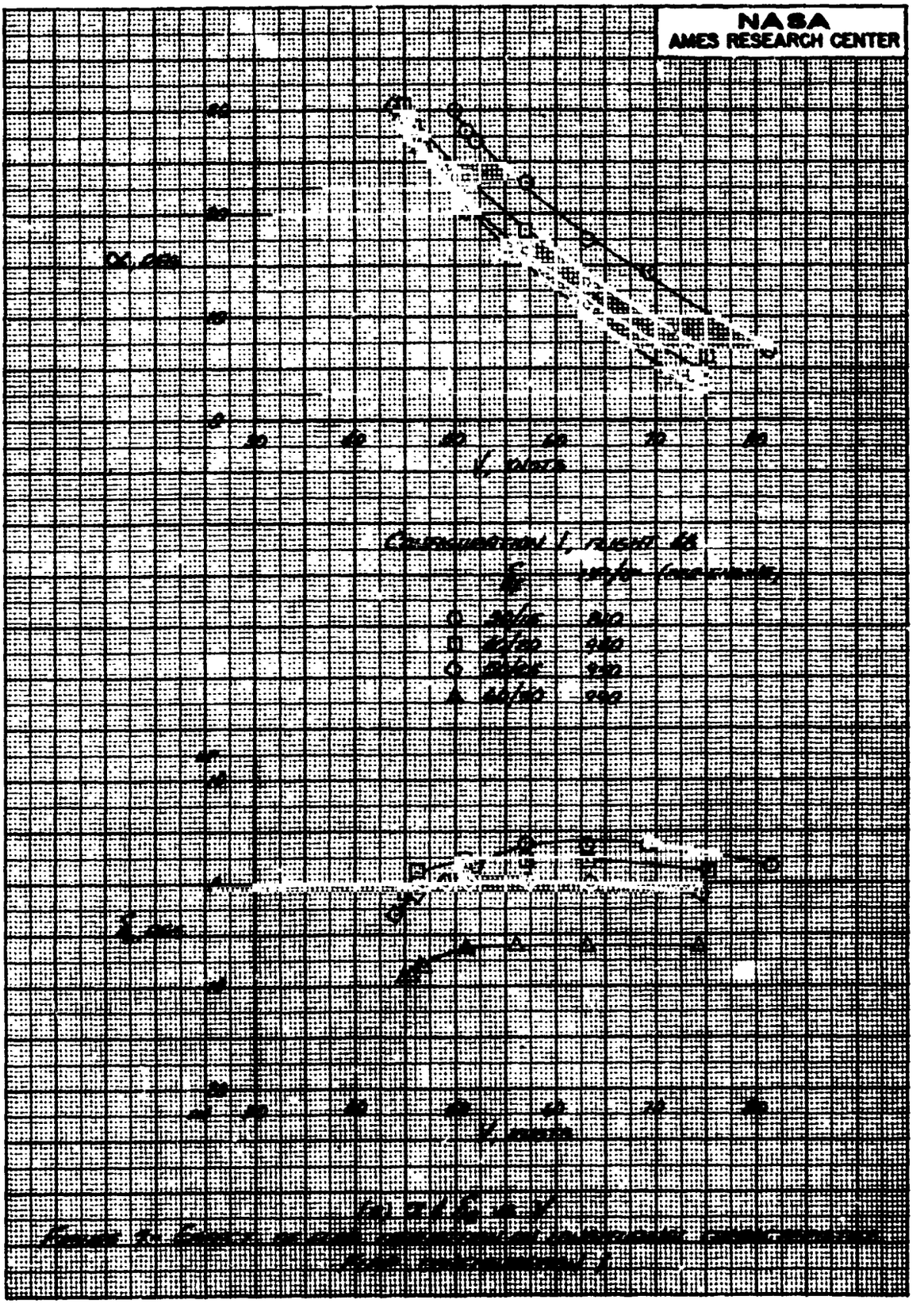
NASA
AMES RESEARCH CENTER

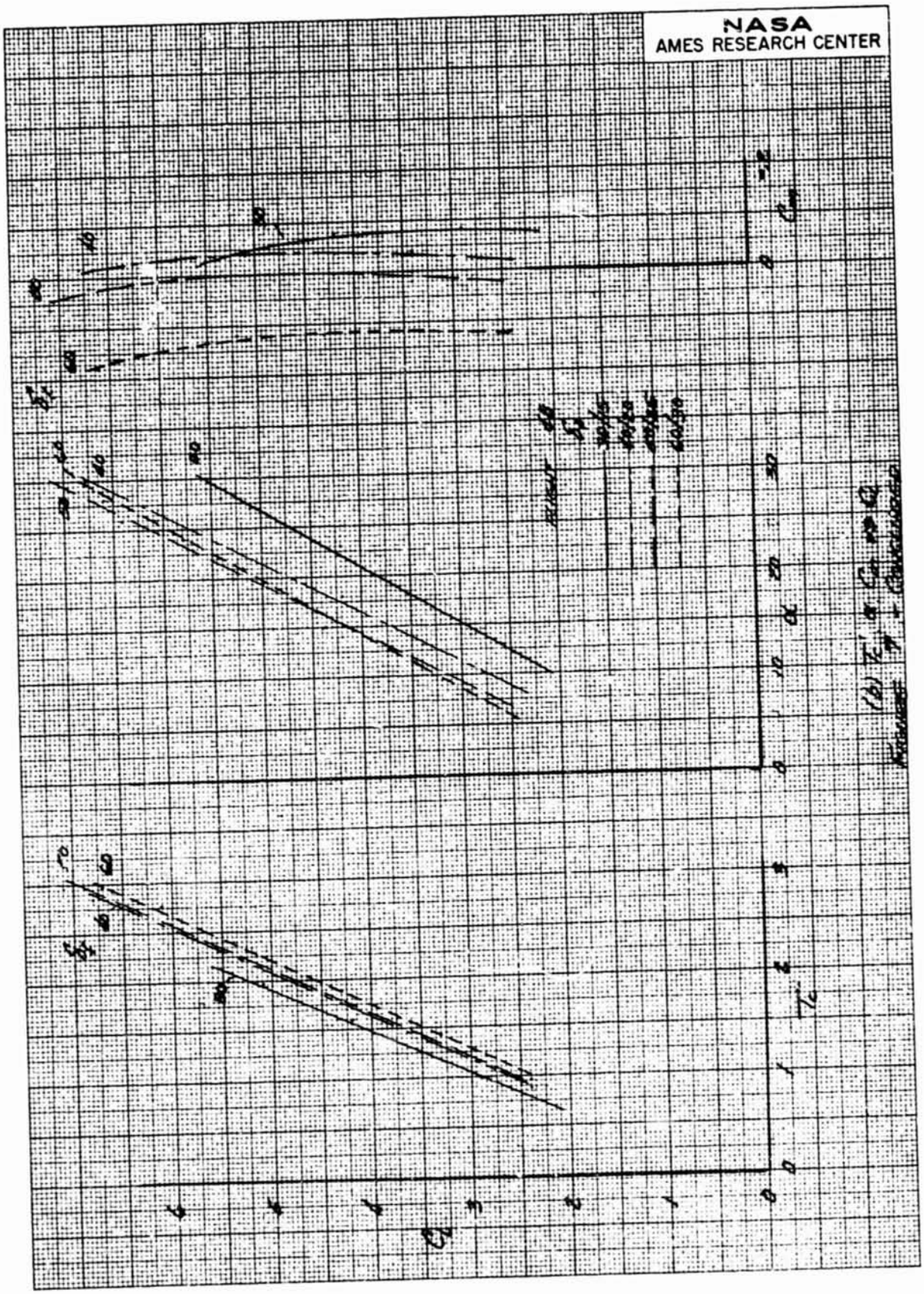
NASA
AMES RESEARCH CENTER

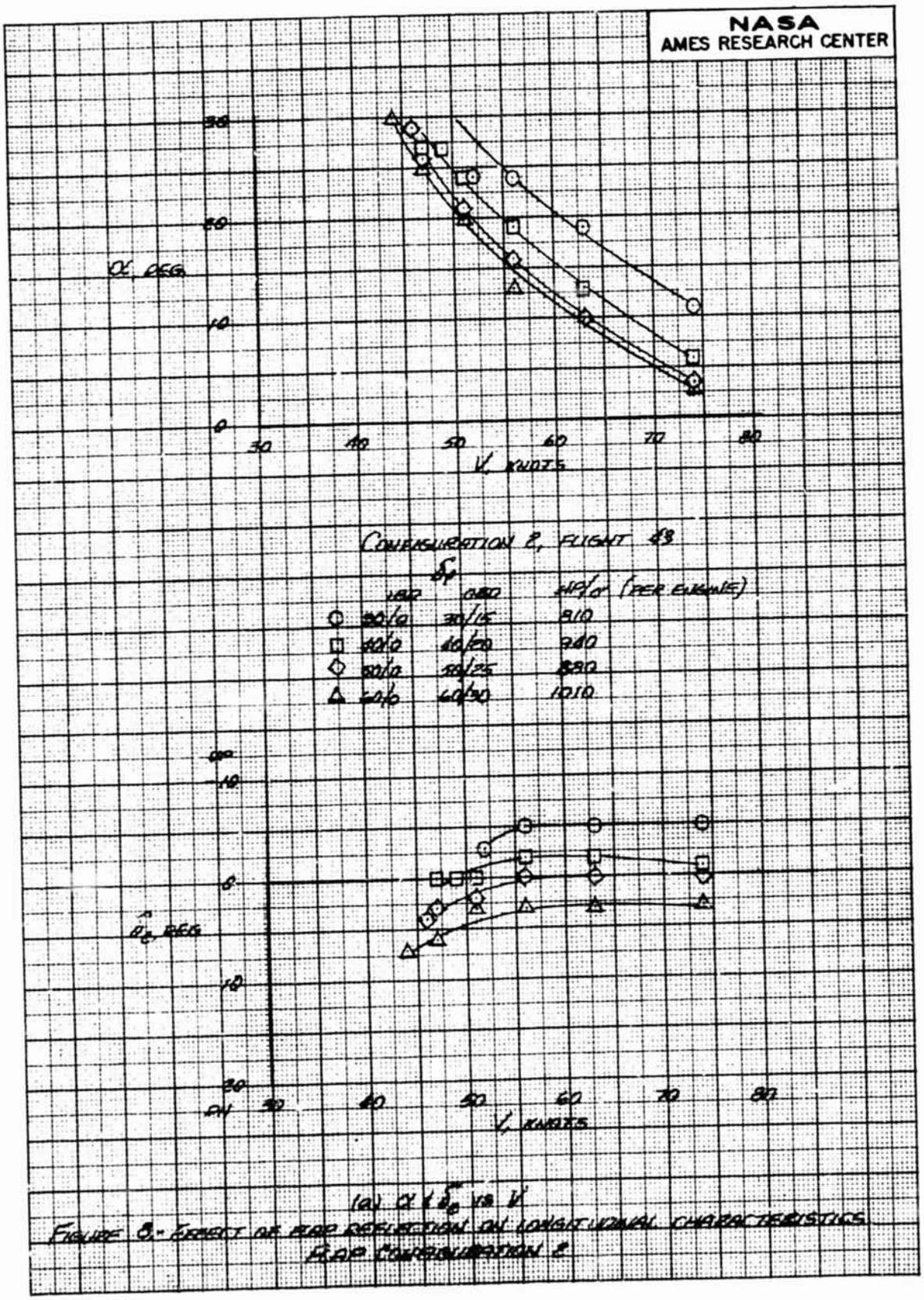

(a) α & δ_e vs V

FIGURE 8.- EFFECT OF FLAP DEFLECTION ON LONGITUDINAL CHARACTERISTICS. FLAP CONFIGURATION 2

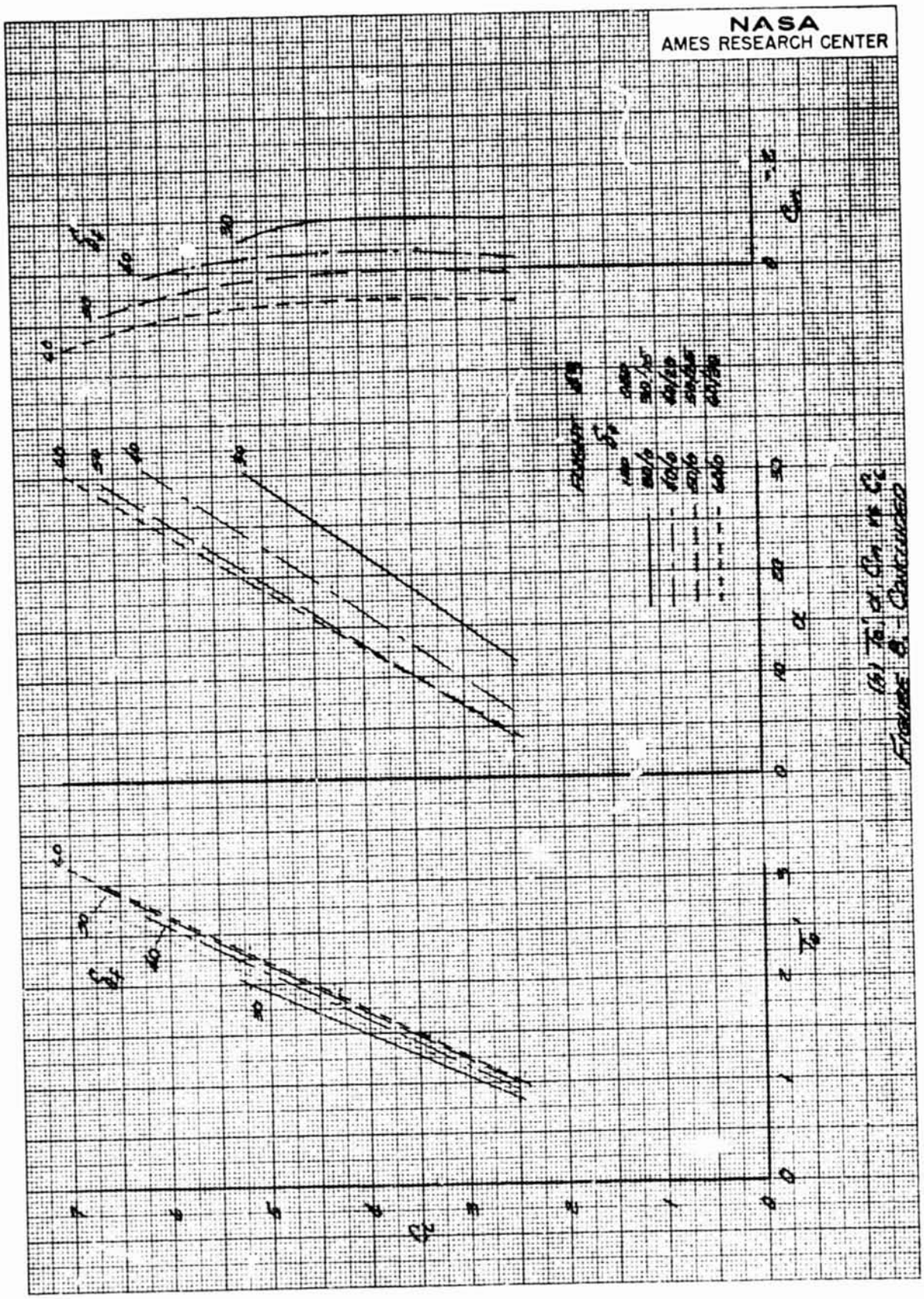
NASA
AMES RESEARCH CENTER

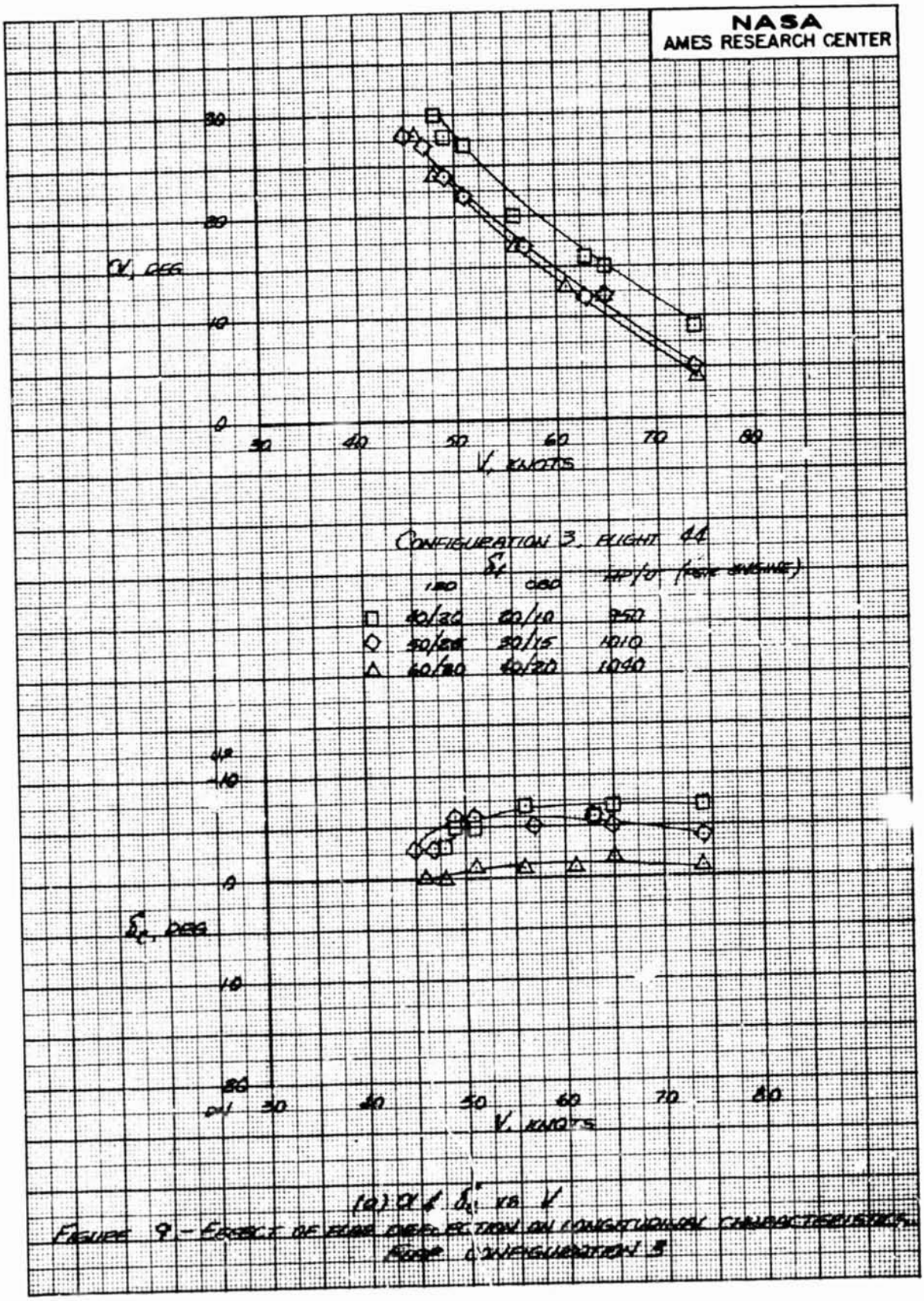

(a) α & δ_e vs V

FIGURE 9 - EFFECT OF FLAP DEFLECTION ON LONGITUDINAL CHARACTERISTICS. FLIGHT CONFIGURATION 3

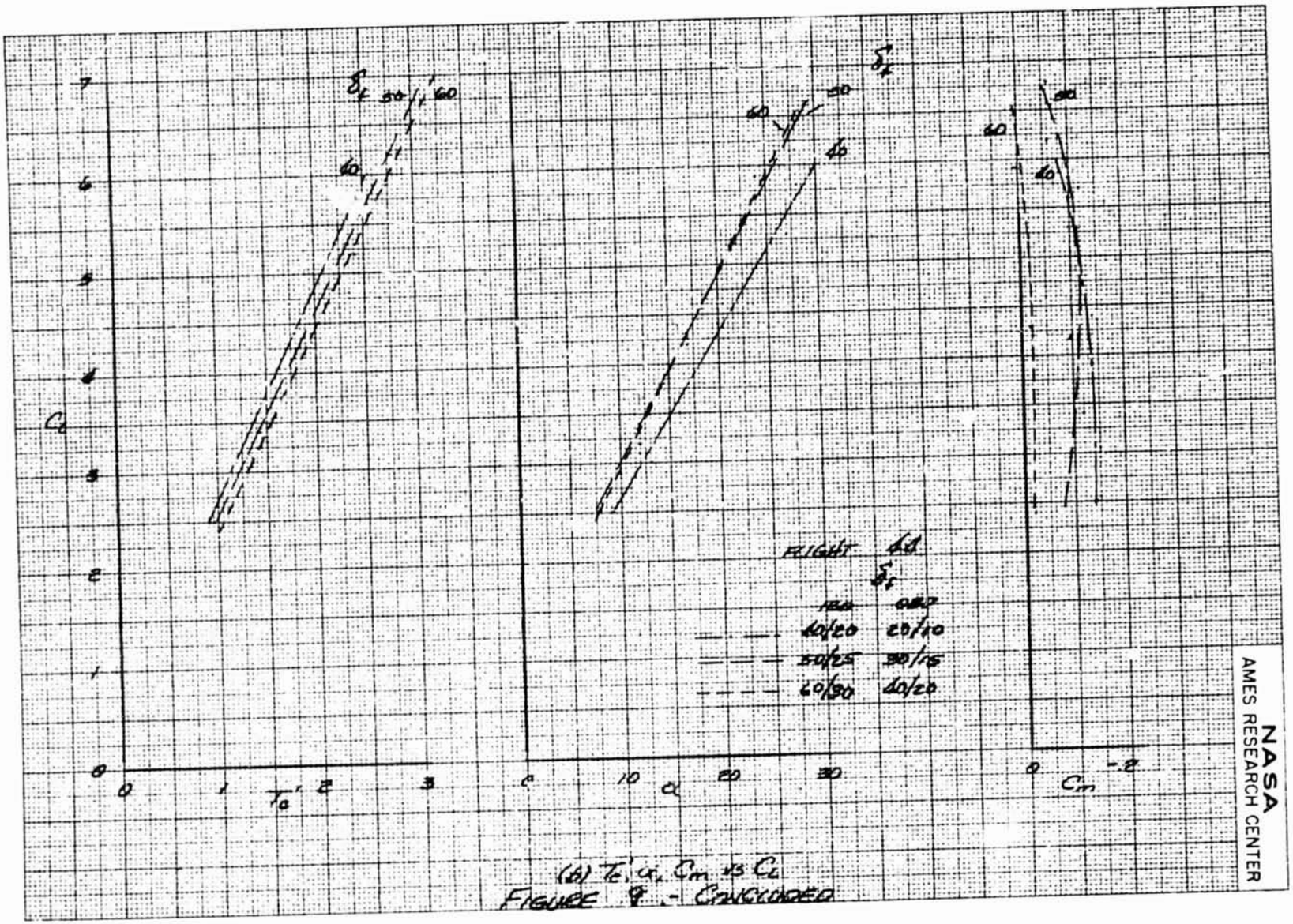

(b) T_c, C_L, C_m vs C_L

FIGURE 9.- CONCLUDED

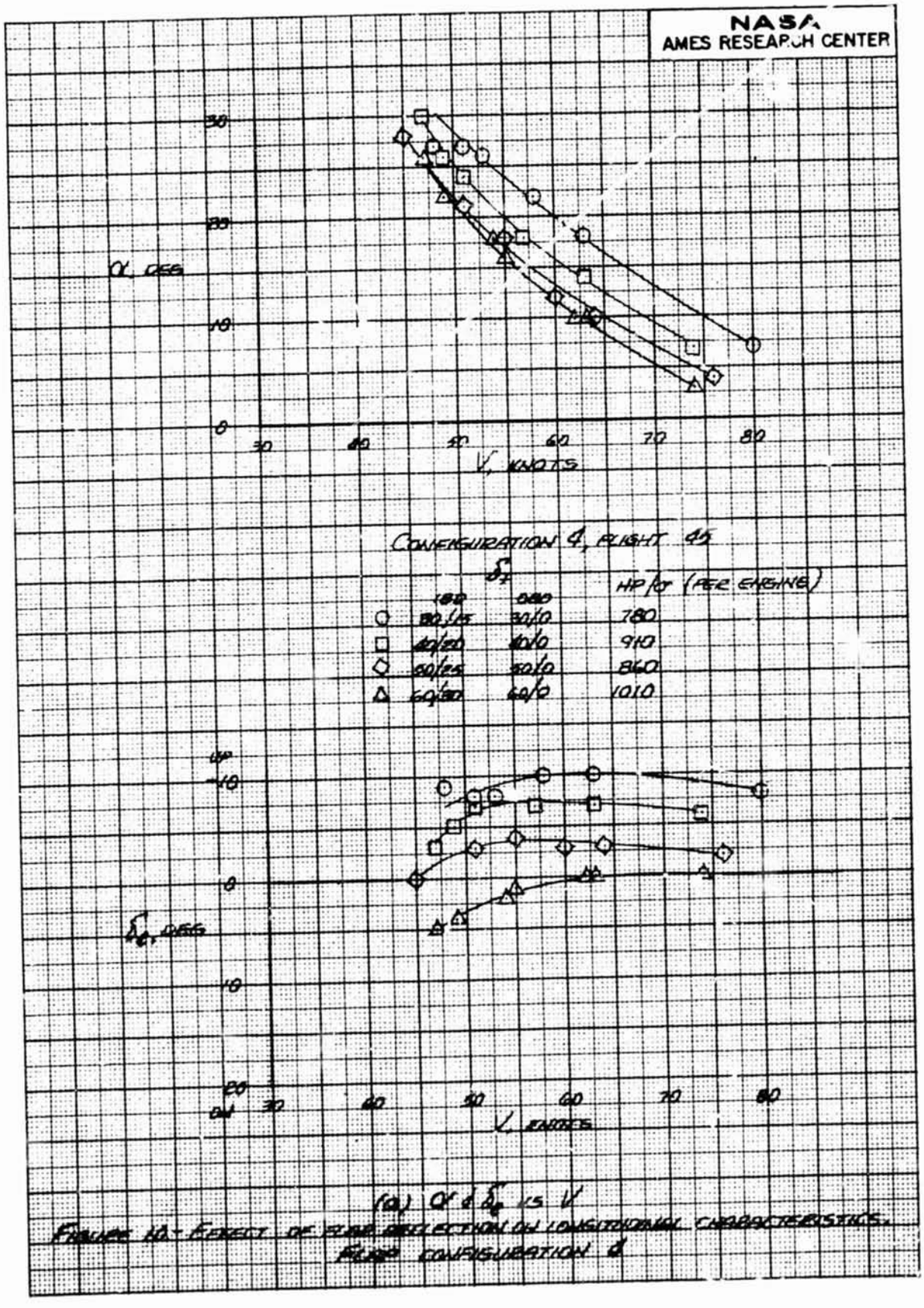

(a) α or δ_e vs V

FIGURE 40.- EFFECT OF FLAP DEFLECTION ON LONGITUDINAL CHARACTERISTICS. FLIGHT CONFIGURATION 4

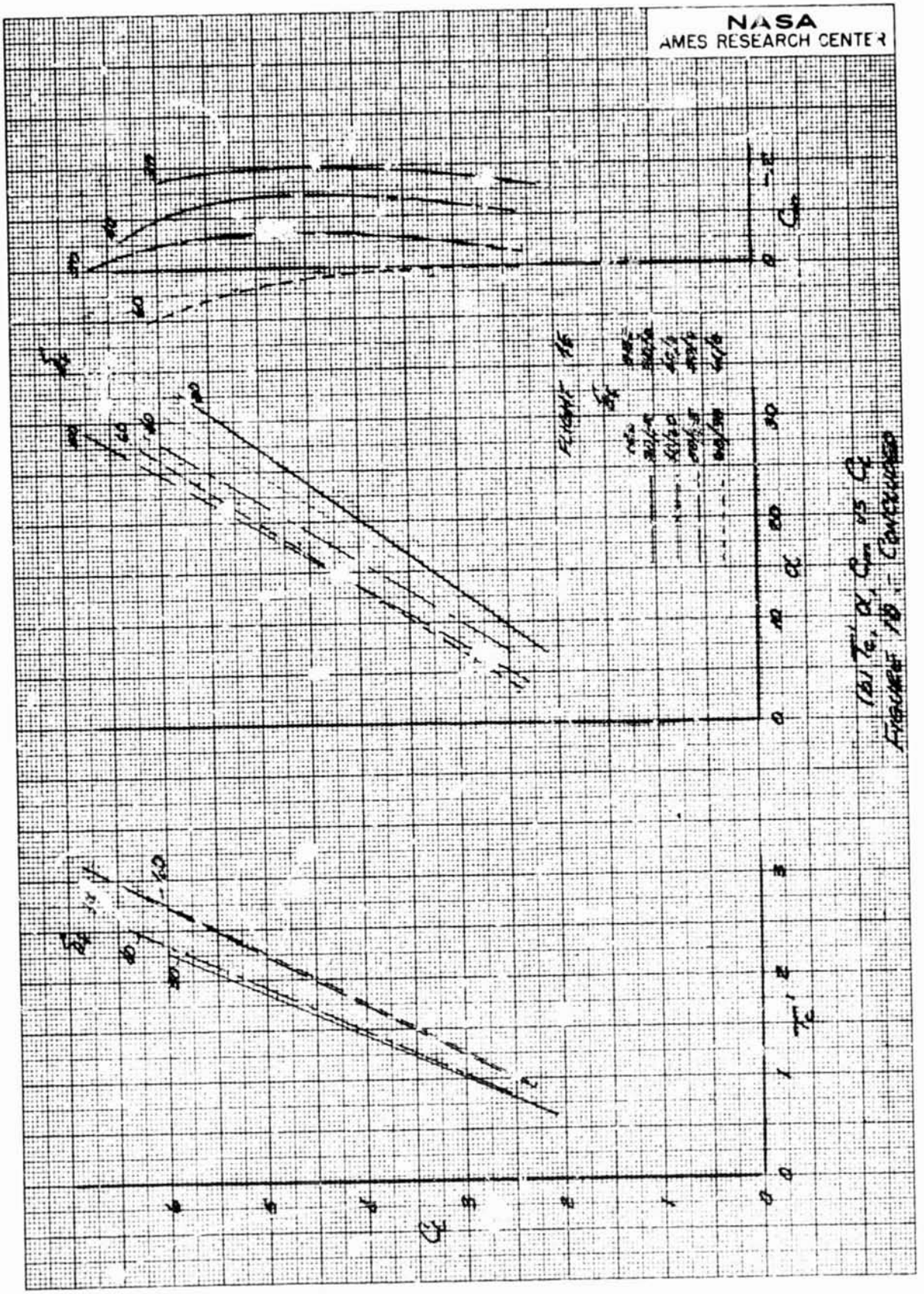
NASA
AMES RESEARCH CENTER

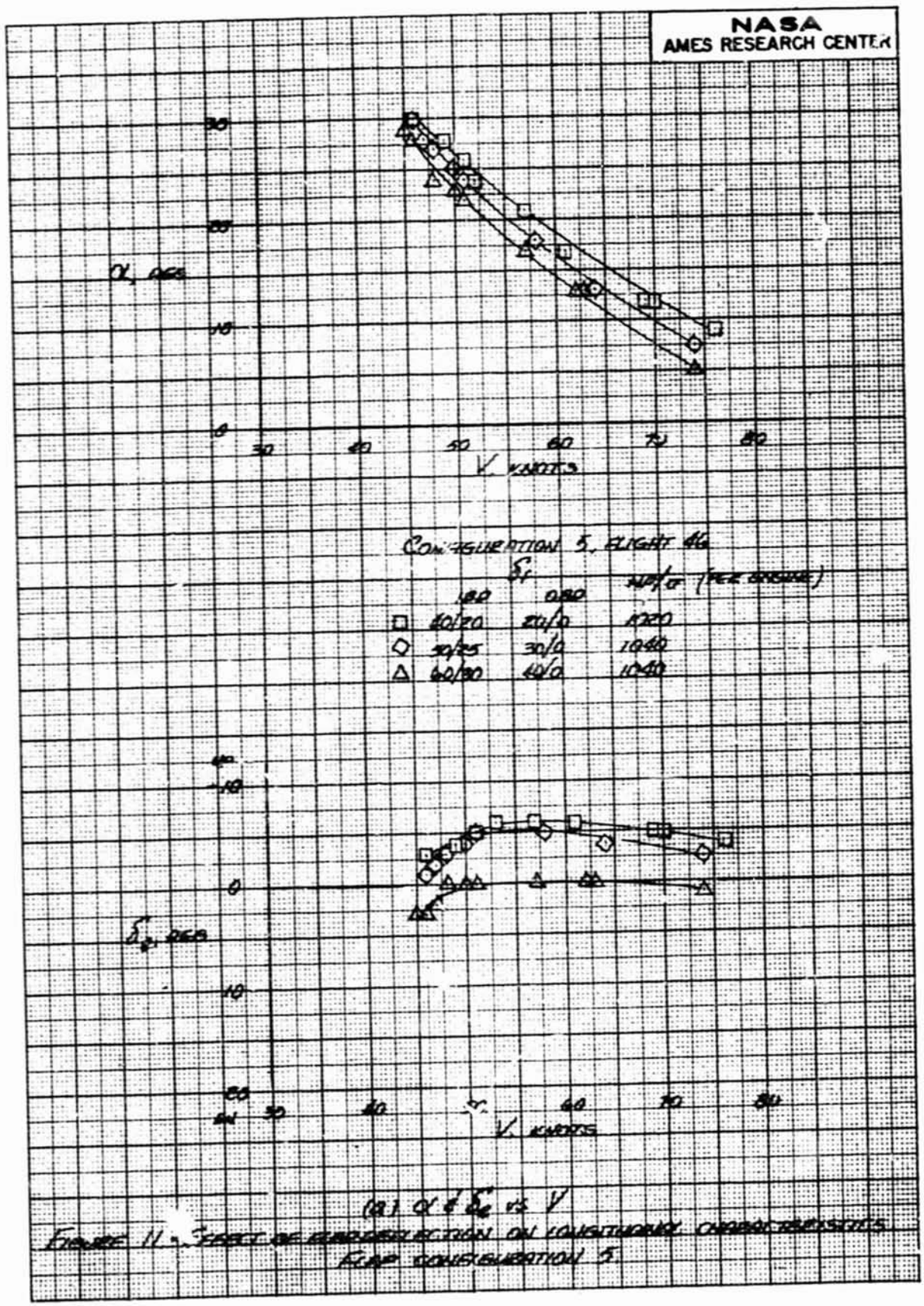

(a) α & δ_e vs V

FIGURE 11.- EFFECT OF REINGESTION ON LONGITUDINAL CHARACTERISTICS. FLAP CONFIGURATION 5.

NASA
AMES RESEARCH CENTER

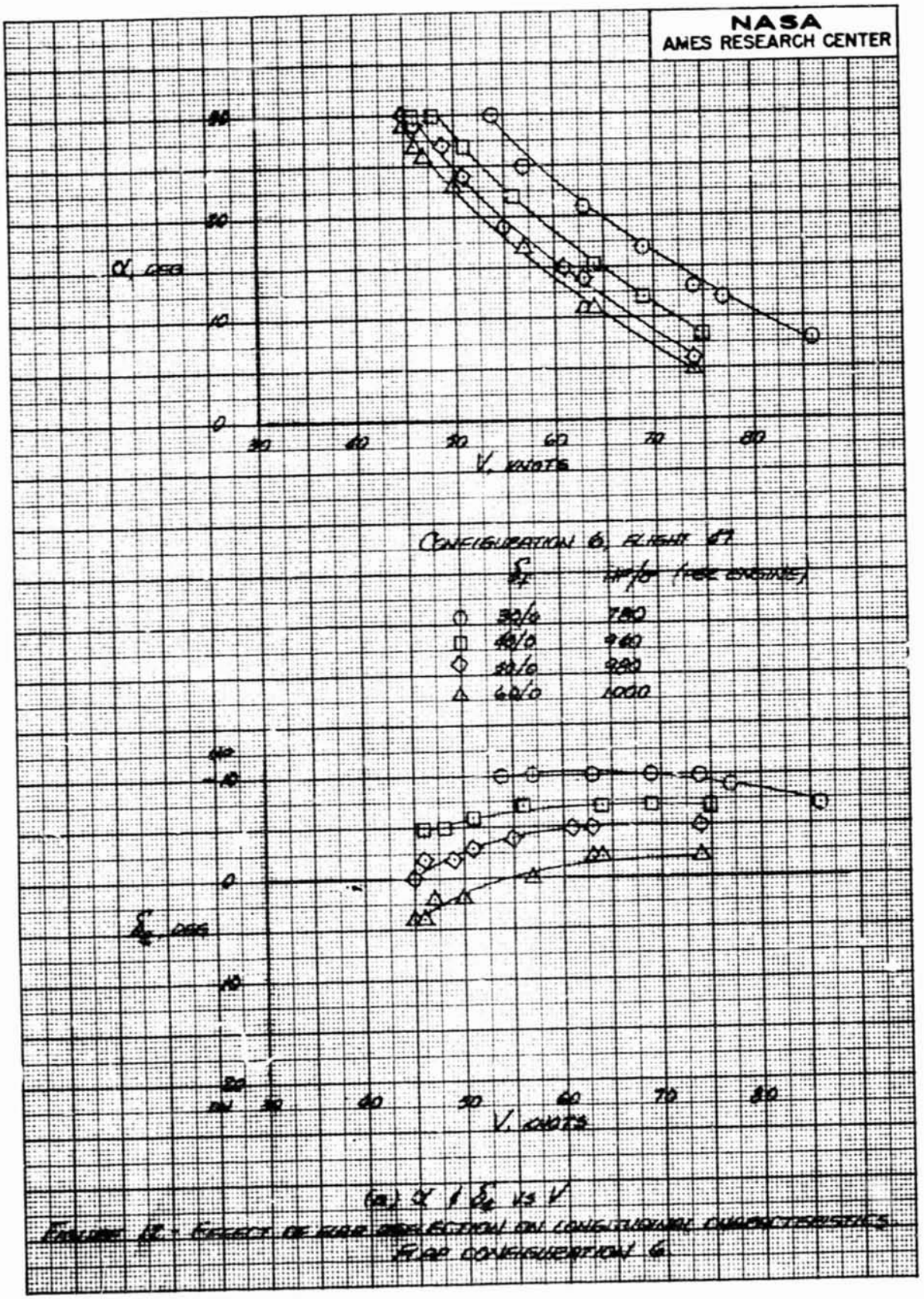

(a) α & δ_e vs V

FIGURE 12 - EFFECT OF FLAP DEFLECTION ON LONGITUDINAL CHARACTERISTICS FOR CONFIGURATION 6

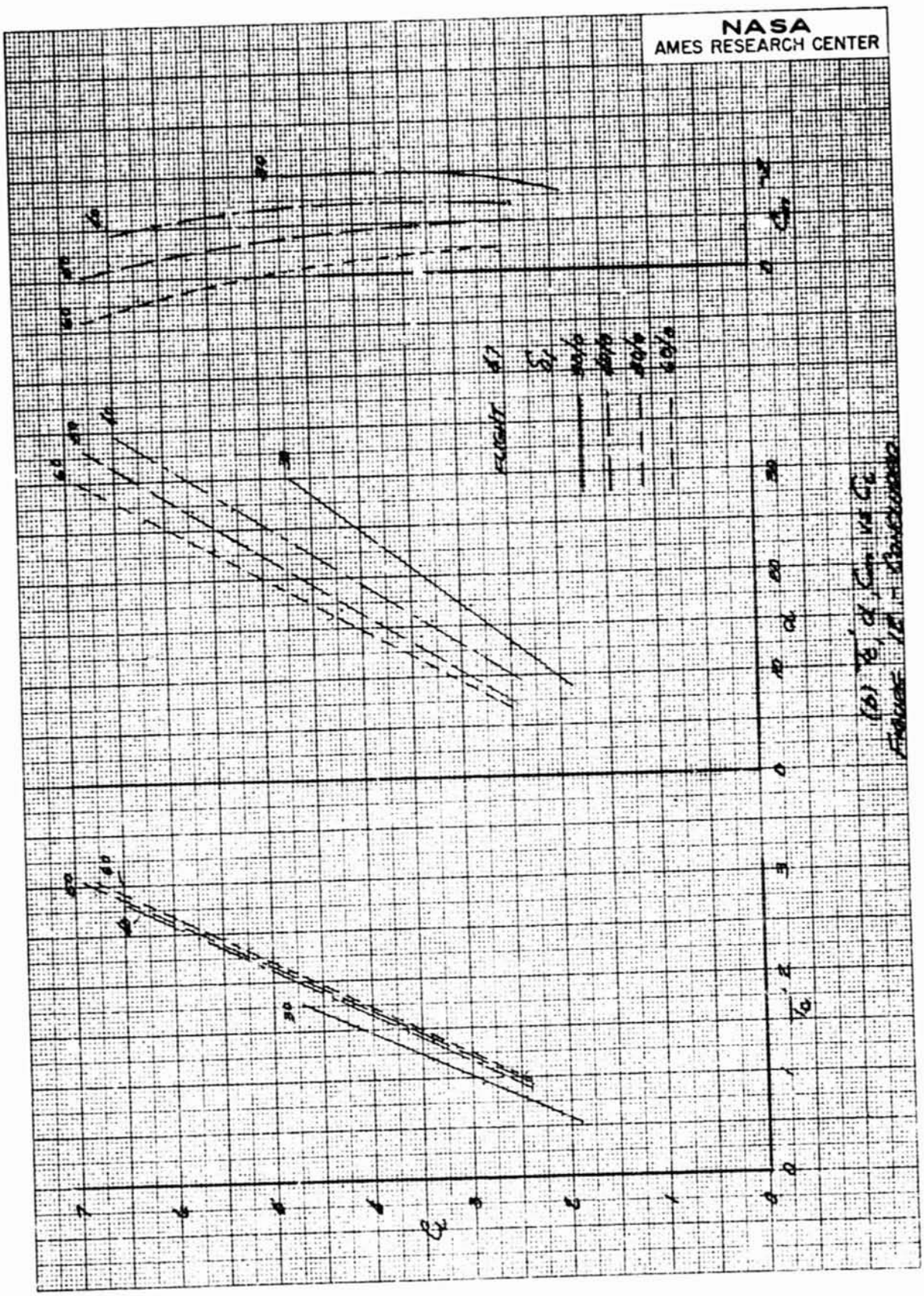
NASA
AMES RESEARCH CENTER

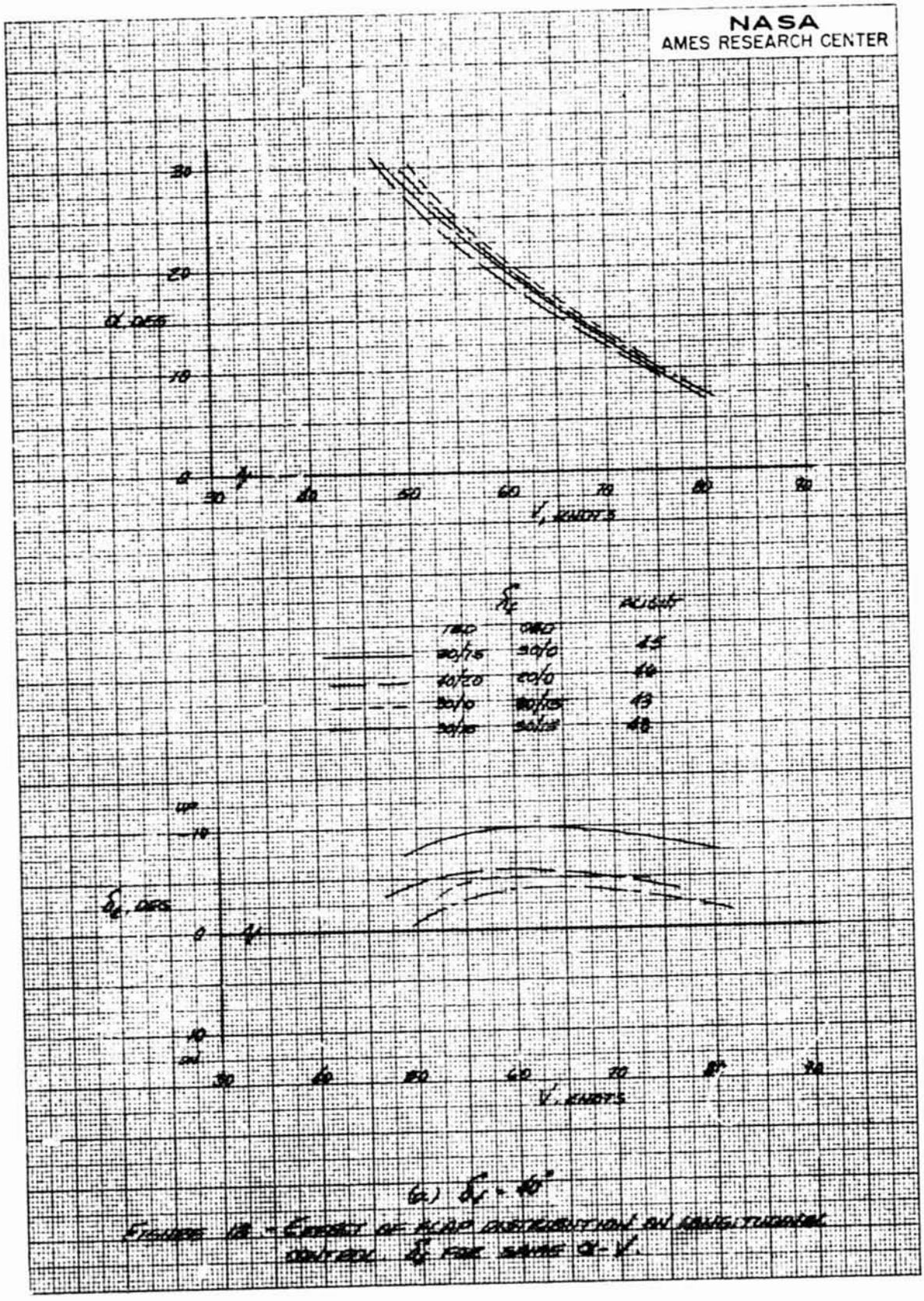

(a) $\delta_f = 40°$

FIGURE 18.- EFFECT OF FLAP DEFLECTION ON LONGITUDINAL CONTROL, δ_f FOR TRIM OF V.

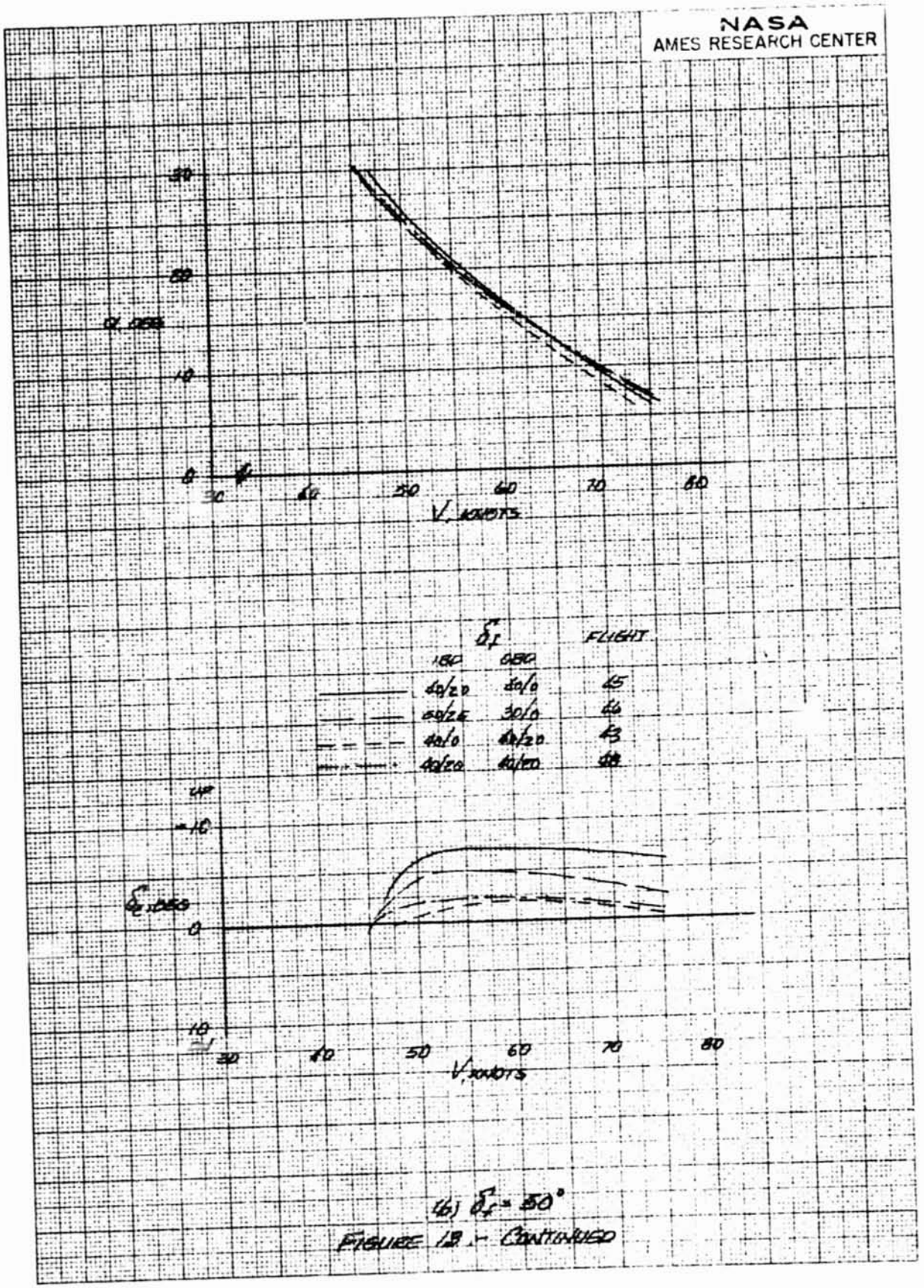

(b) $\delta_f = 50°$

FIGURE 12 - CONTINUED

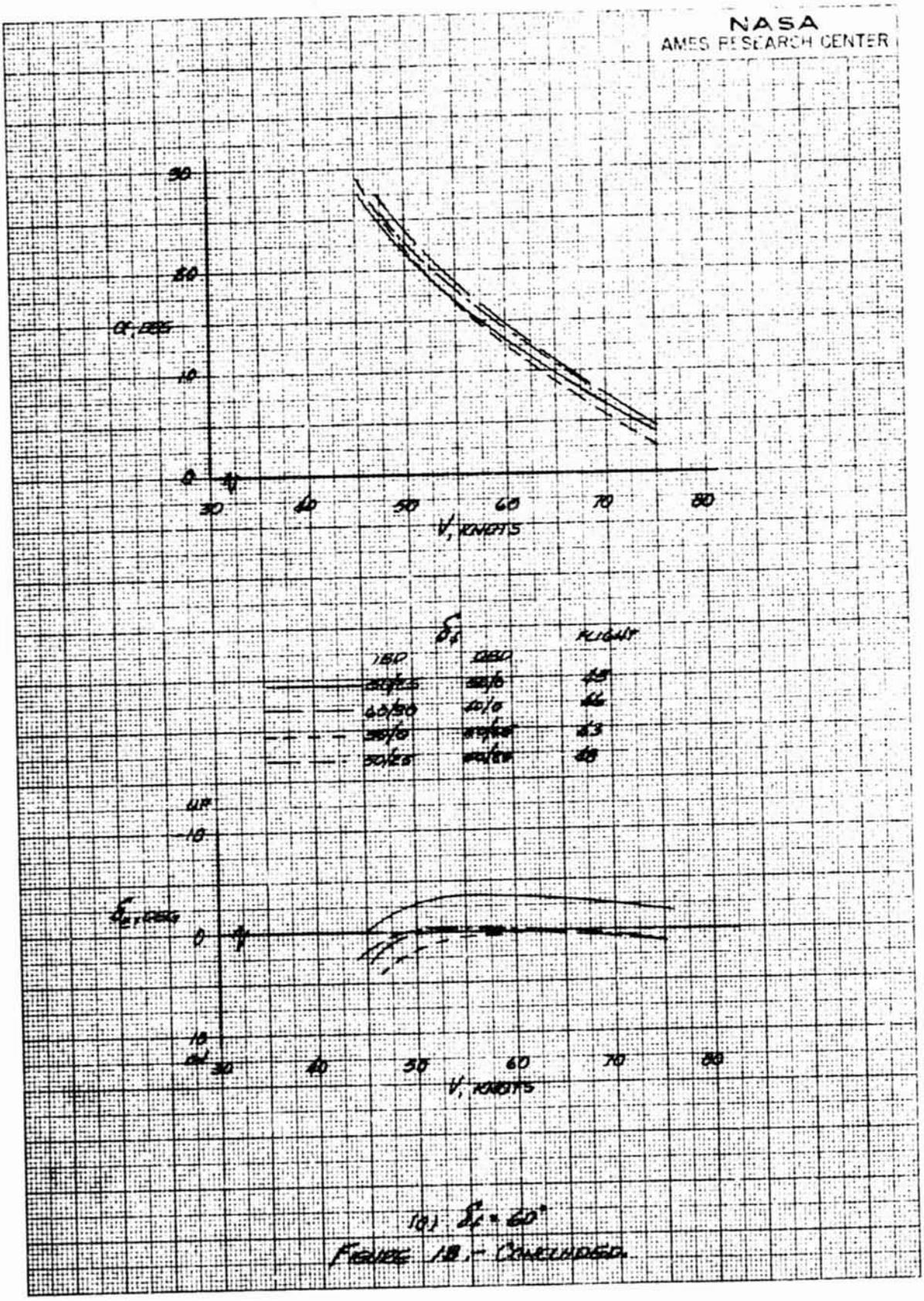

(a) $\delta_f = 60°$

FIGURE 18.- CONCLUDED.

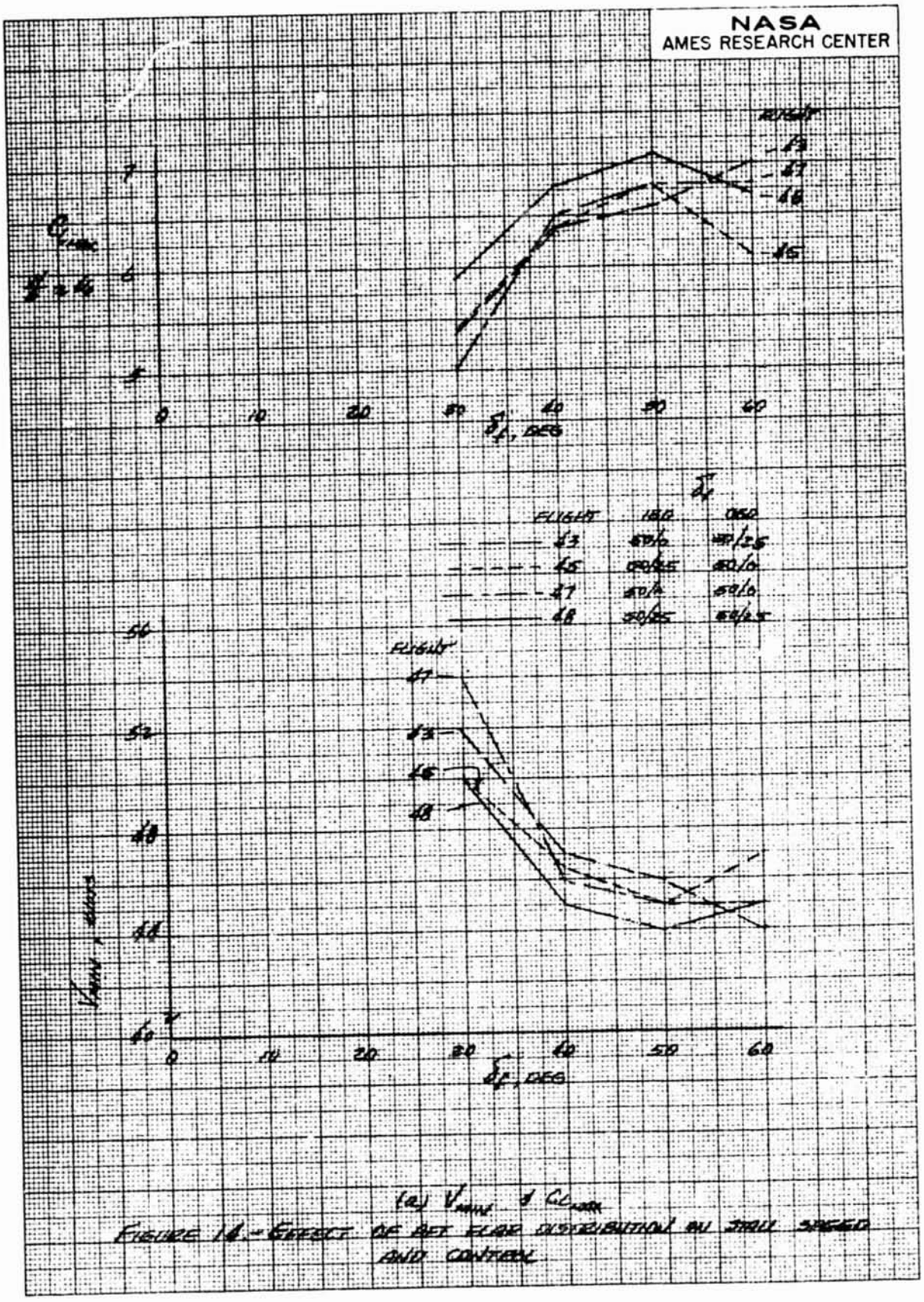

(a) V_{min} and $C_{L_{max}}$

FIGURE 18.- EFFECT OF JET FLAP DISTRIBUTION ON STALL SPEED AND CONTROL

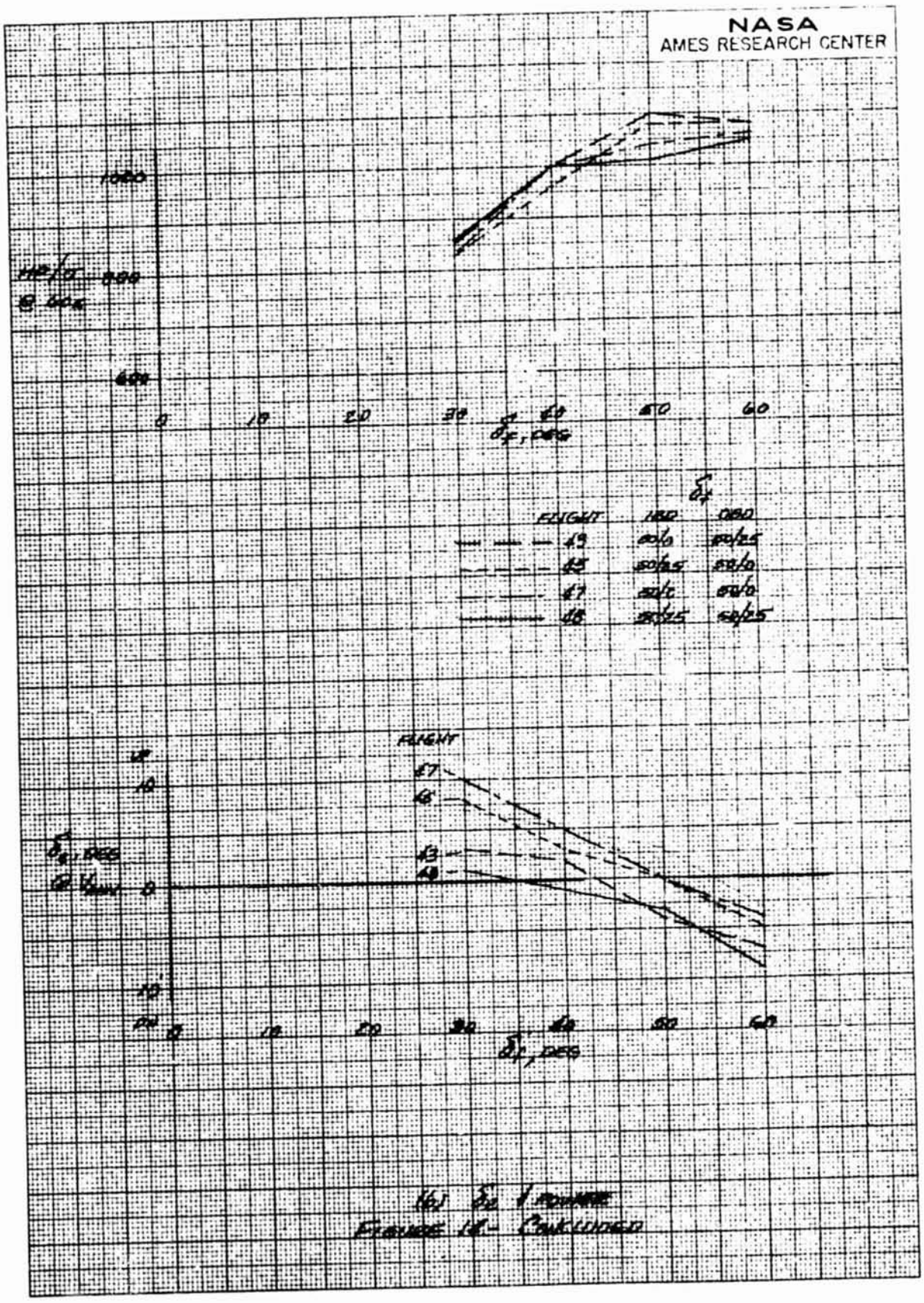
NASA
AMES RESEARCH CENTER
1000
0
10
20
30
40
50
60
FLIGHT
49
45
47
43
48

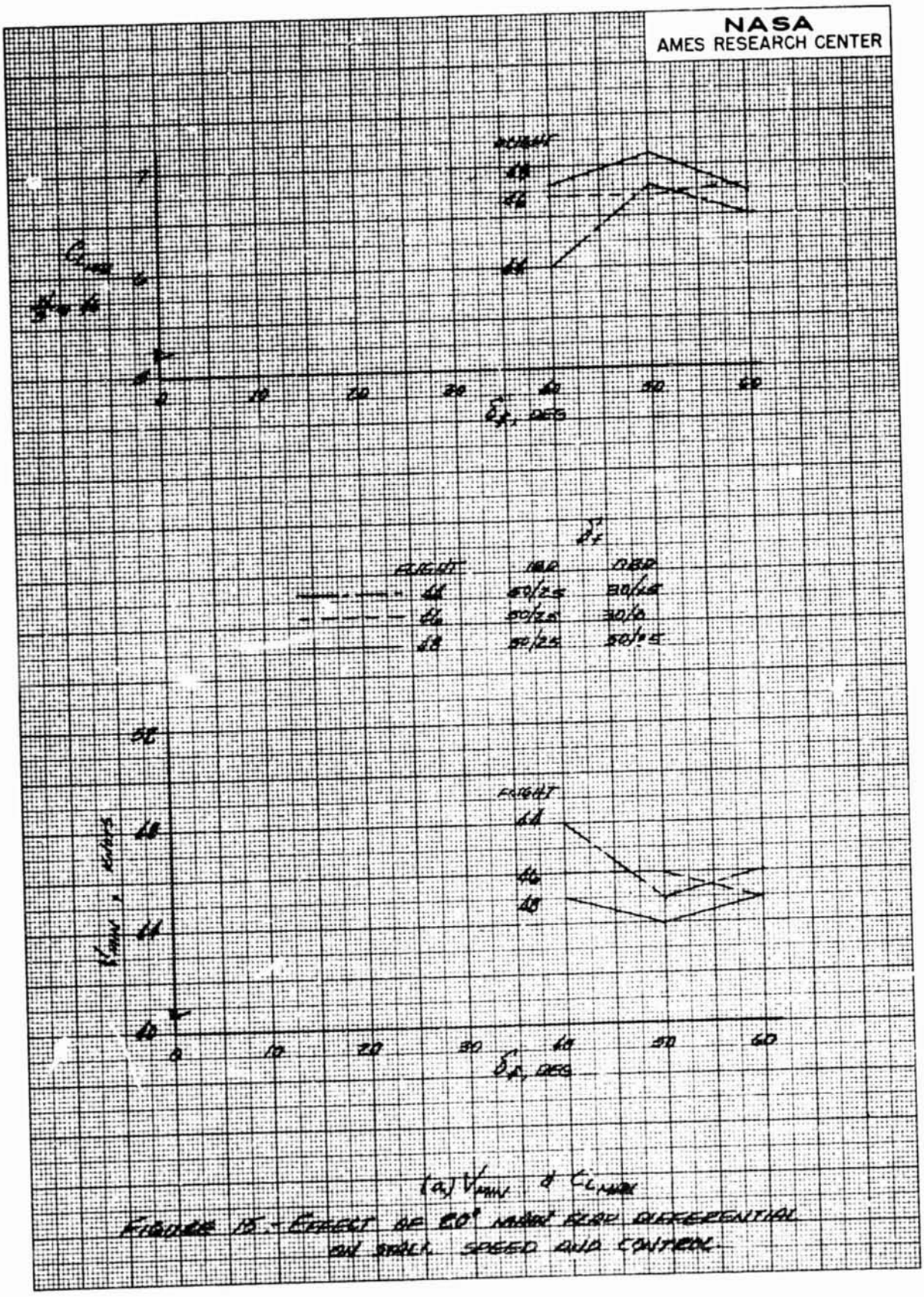

(a) V_{min} & $C_{L_{max}}$

FIGURE 15.- EFFECT OF 60° MAIN REAR DEFLECTION ON STALL SPEED AND CONTROL

NASA
AMES RESEARCH CENTER

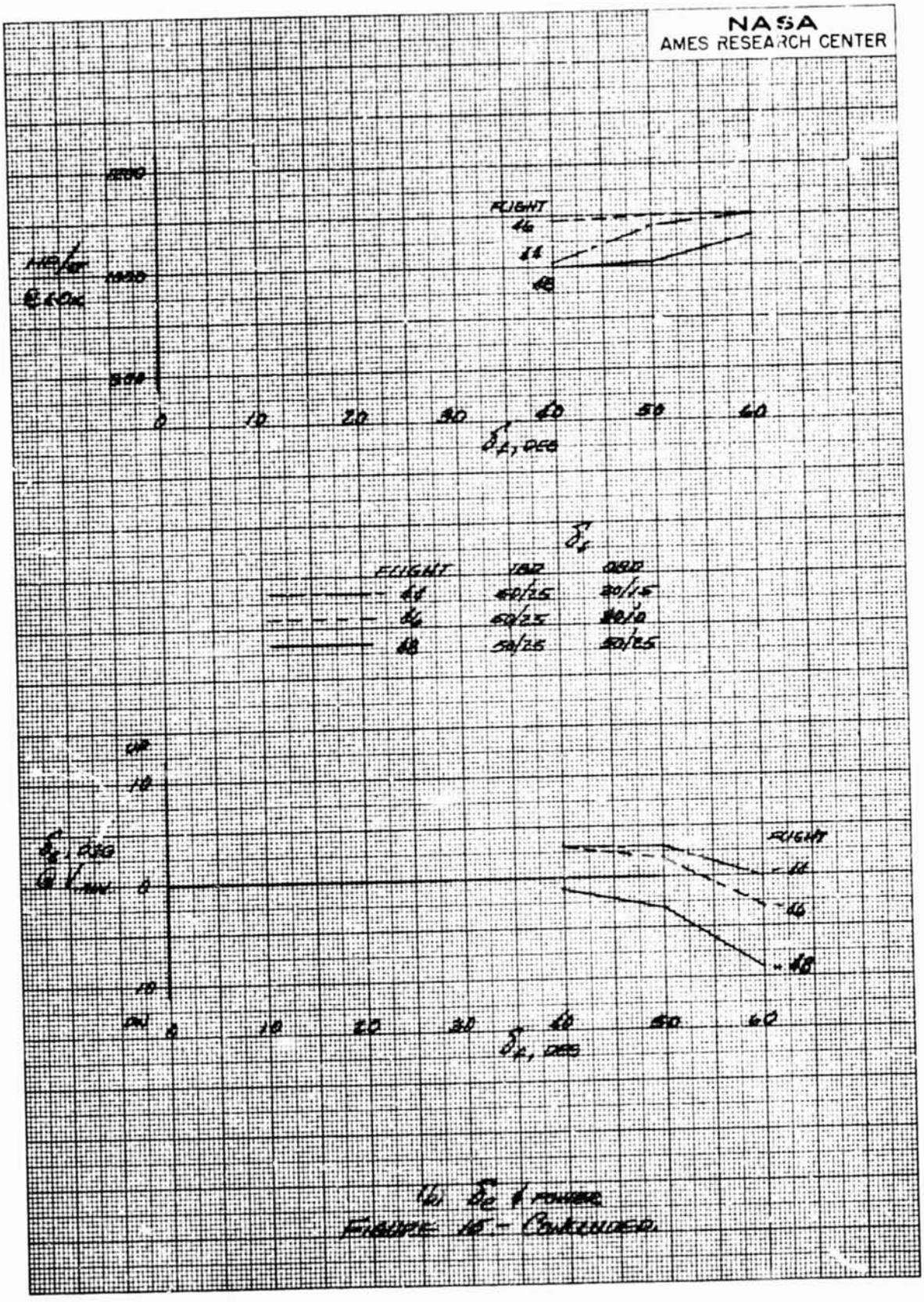

46, δ_f & POWER.

FIGURE 46 - CONCLUDED.

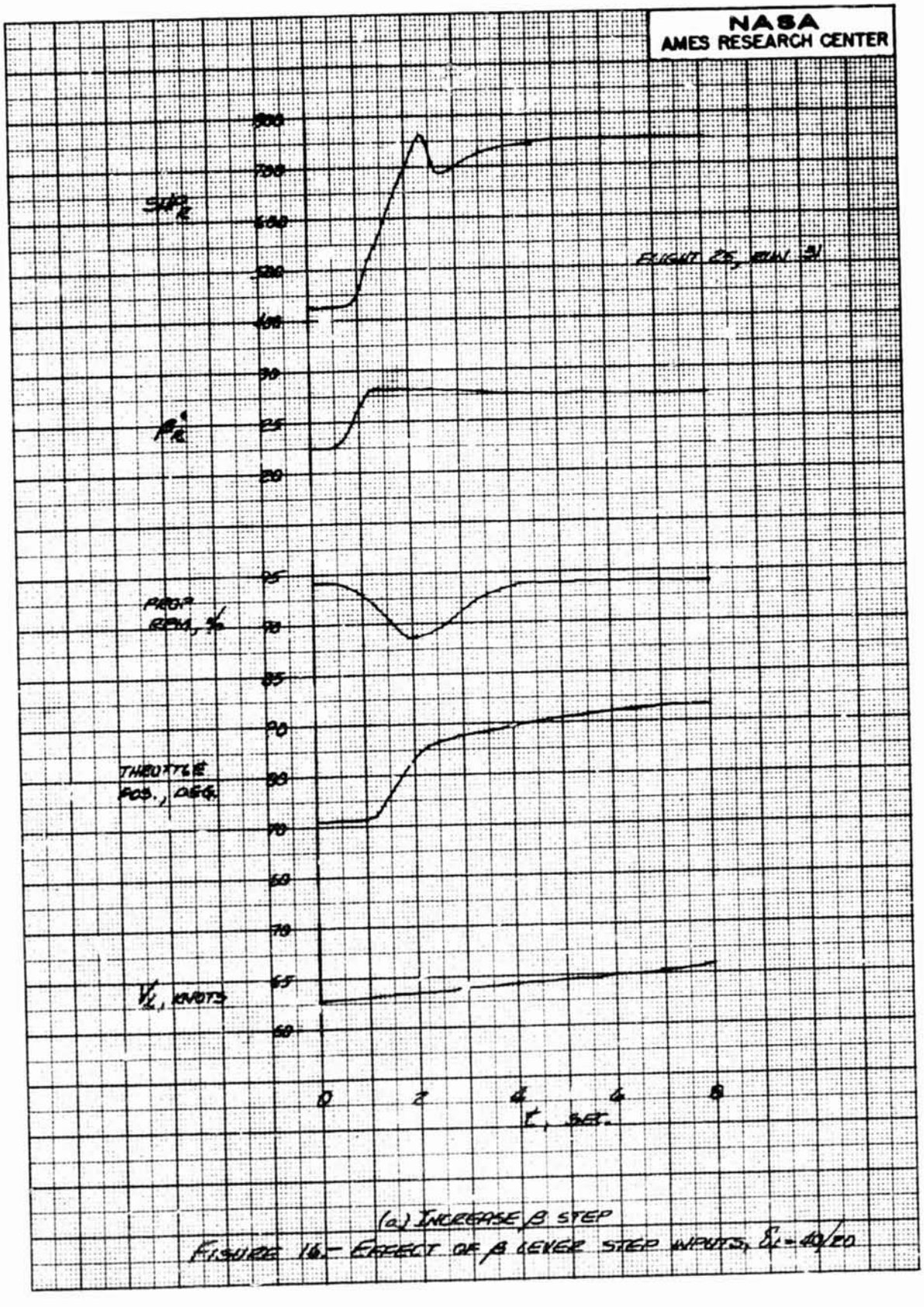

(a) INCREASE, β STEP

FIGURE 16.- EFFECT OF β LEVER STEP INPUTS, $\delta_{\beta_L} = 40/20$

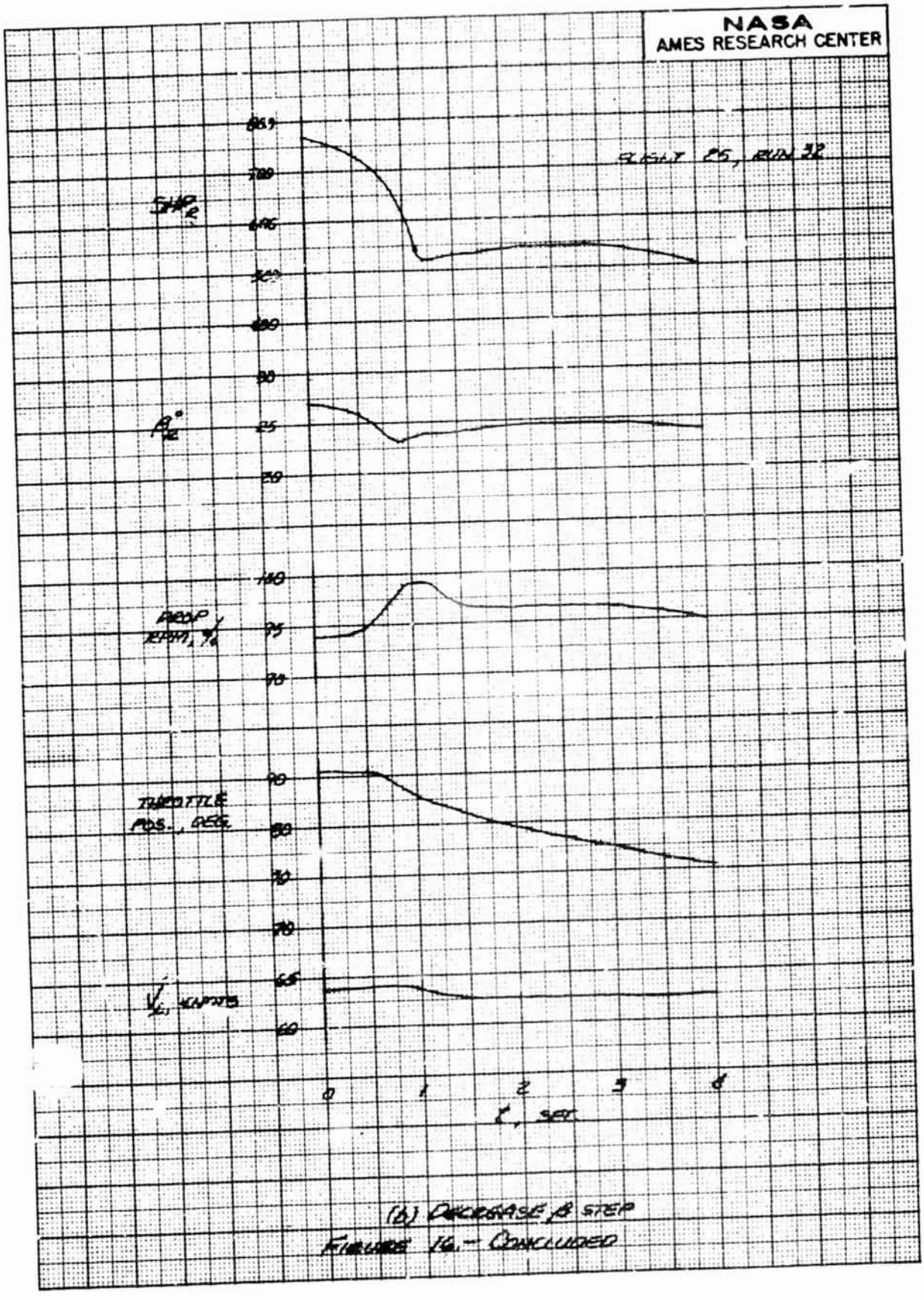

(b) DECREASE, A STEP

FIGURE 16.- CONCLUDED

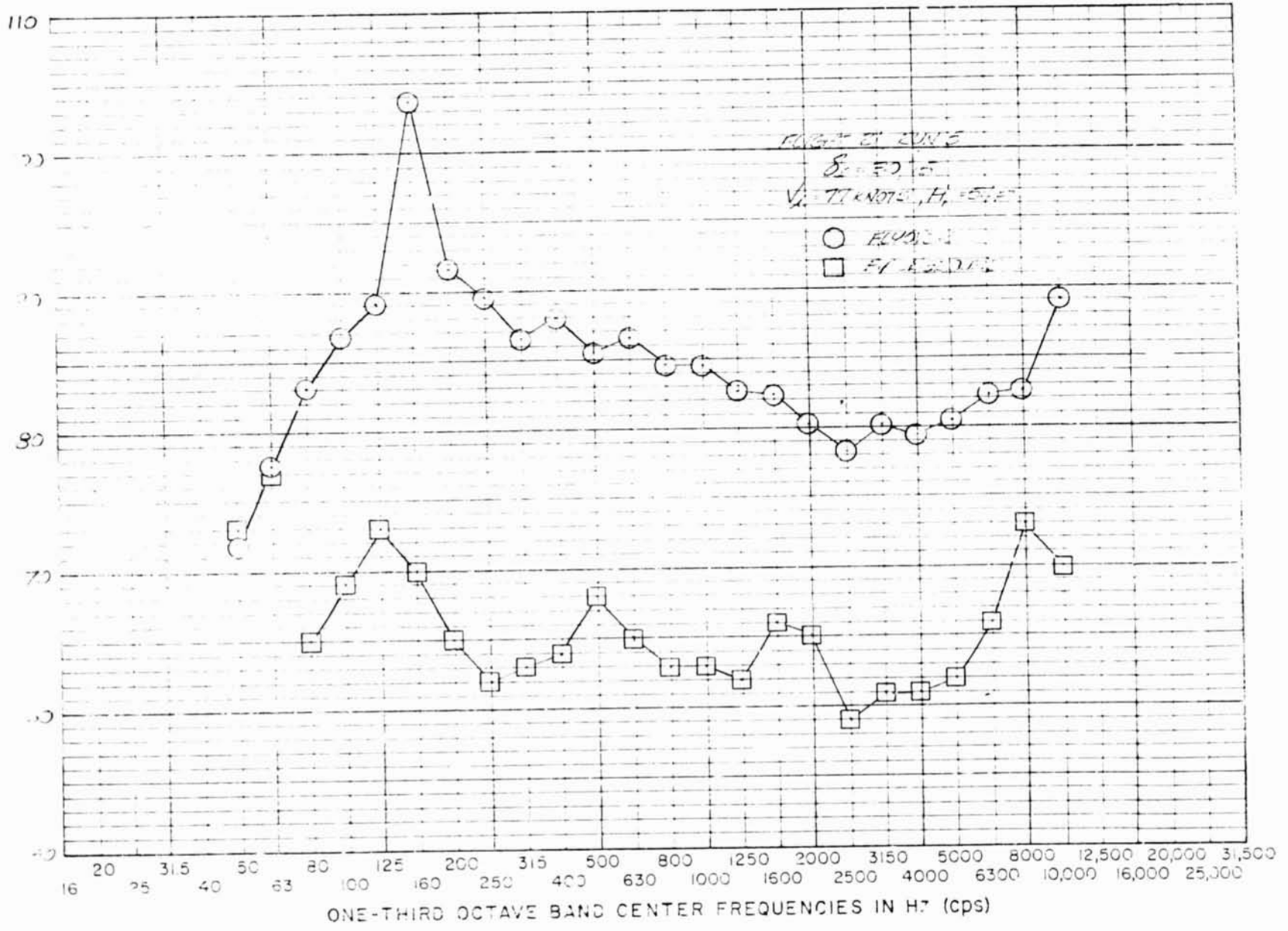

FIGURE 17.- SOUND PRESSURE LEVEL FREQUENCY SPECTRUM.

National Aeronautics and Space Administration
Ames Research Center
Moffett Field, Calif

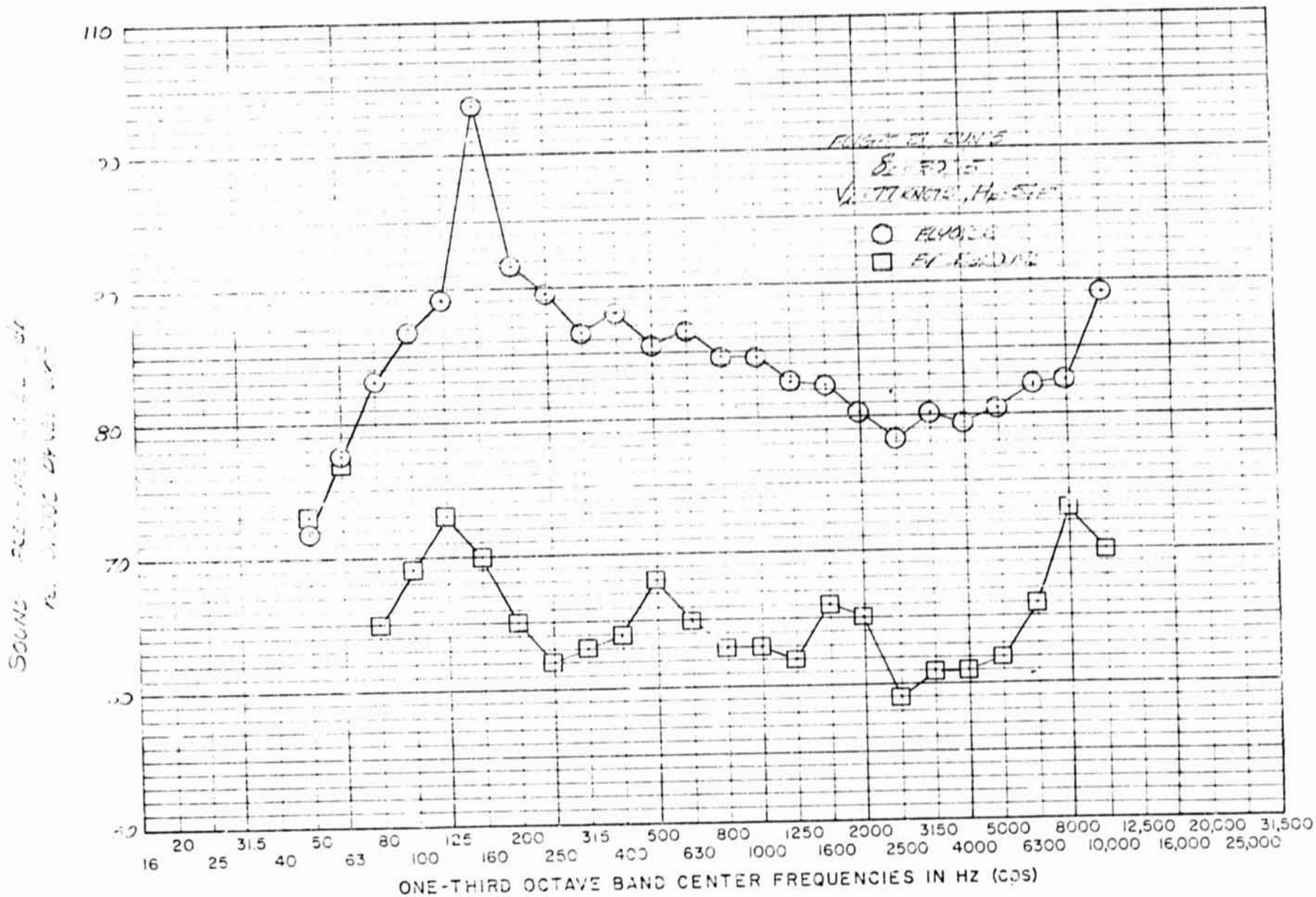

FIGURE 17.- SOUND PRESSURE LEVEL FREQUENCY SPECTRUM.

National Aeronautics and Space Administration
Ames Research Center
Moffett Field, Calif

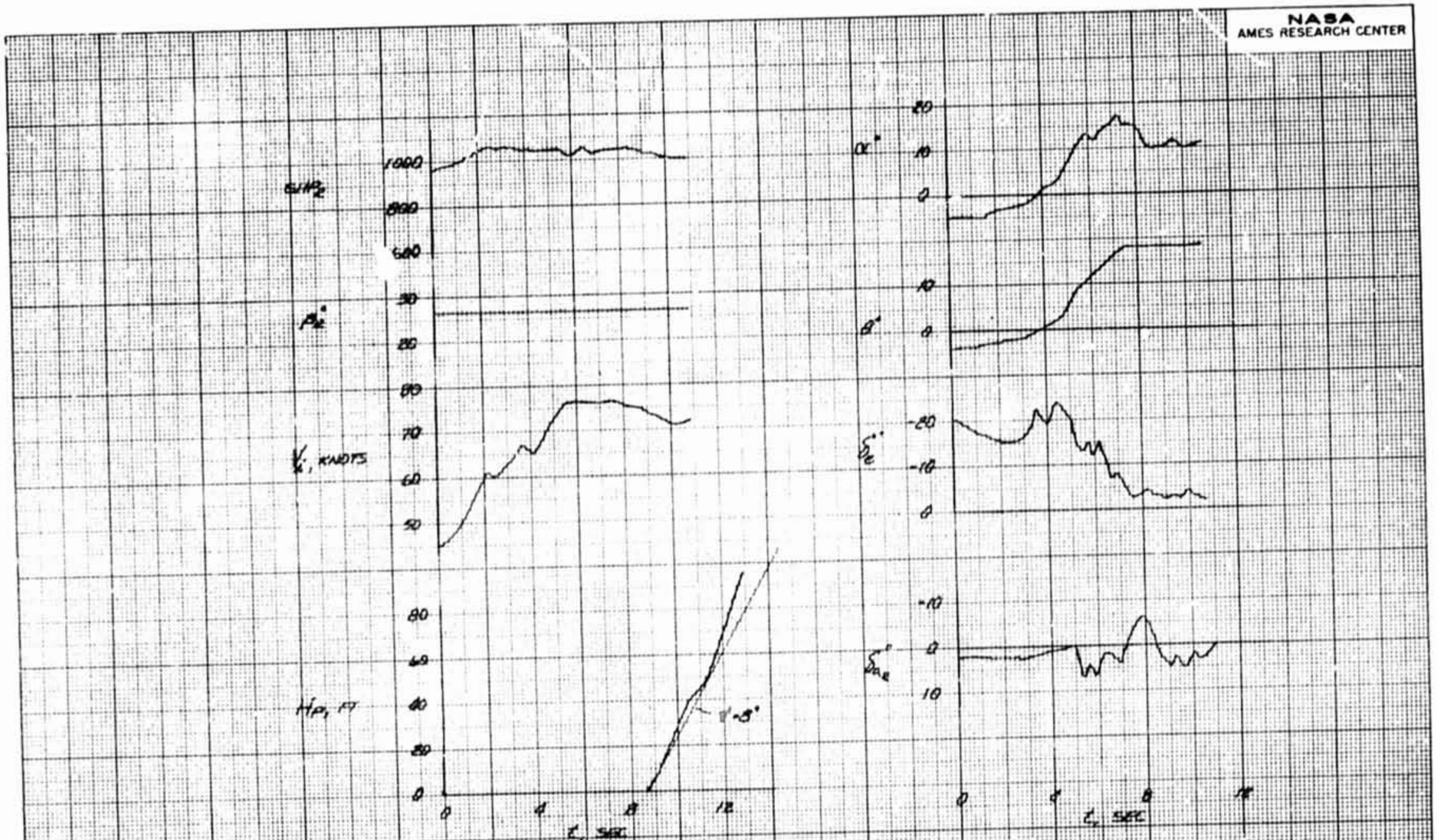

(a) Take off δ_f = 20/10, flight 33, run 2

FIGURE 16.- TIME HISTORIES OF TAKE OFF AND LANDINGS.

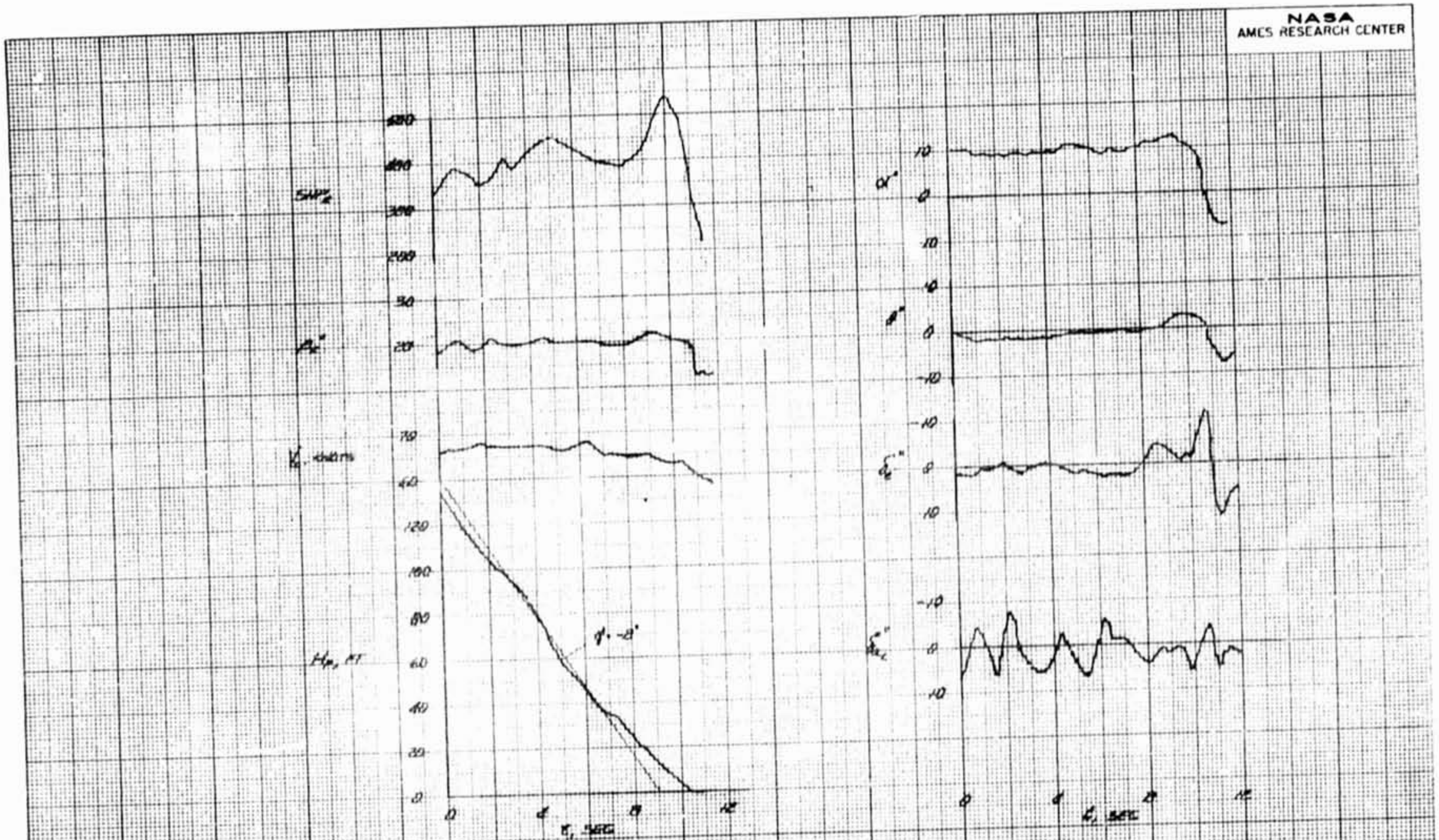

(e) Canards, δ_c = -10/25, flight 22, run 4

Figure 12.- Concluded.

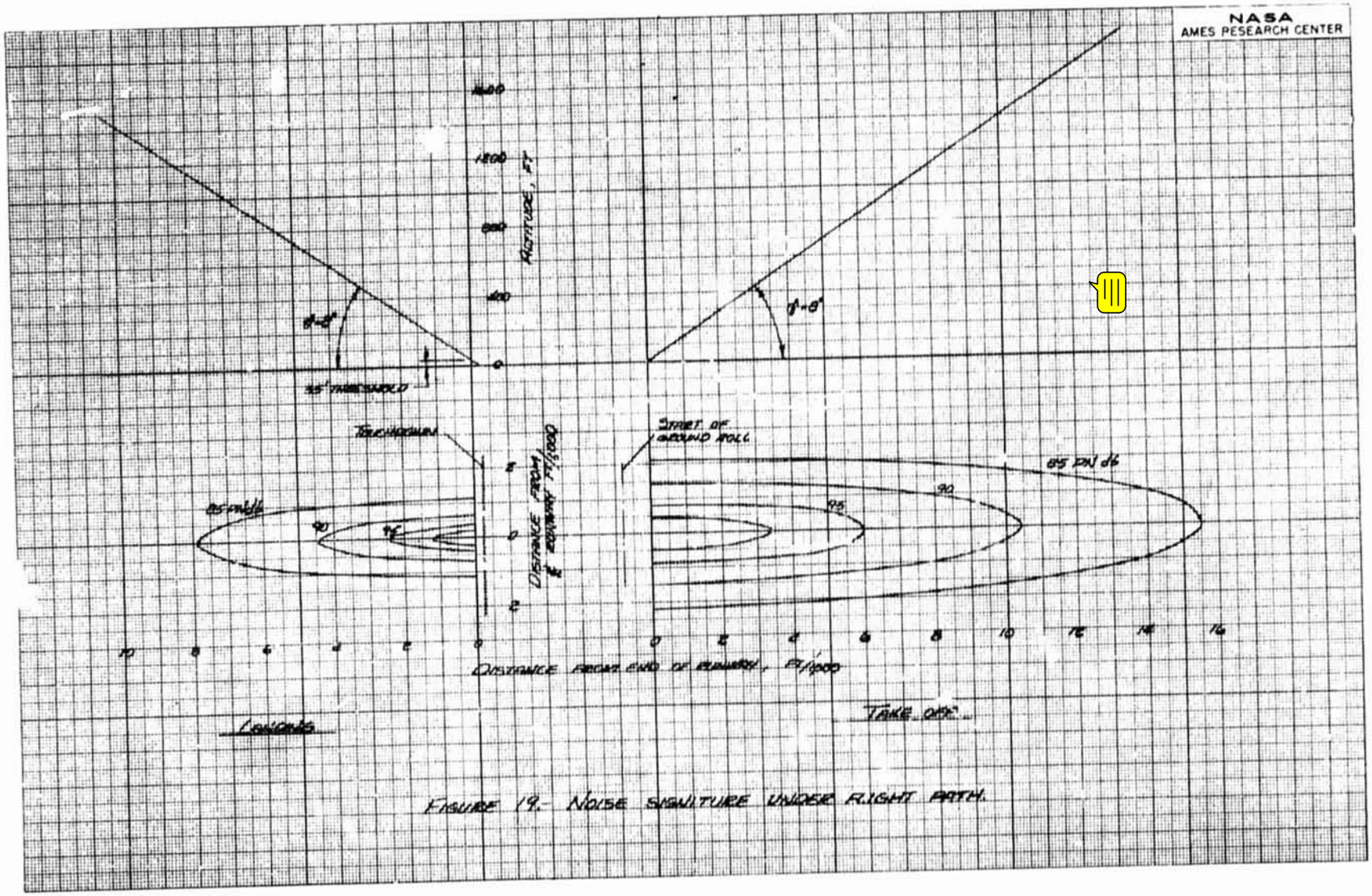

FIGURE 19.- NOISE SIGNATURE UNDER FLIGHT PATH.